

Synthesis and characterization of nickel NiFe₂O₄ nanoparticles by wet chemical sol-gel method



By:

Waqas Shoukat
(289-FBAS/MSPHY/F14)

Supervisor:

Dr. Syed Salman Hussain

Assistant Professor
Department of Physics, FBAS, IIUI

Co-Supervisor:

Dr. Kashif Nadeem

Assistant Professor
Department of Physics, FBAS, IIUI

Department of Physics
Faculty of Basic and Applied Sciences
International Islamic University, Islamabad
(2017)





Accession No TH:18387 *PKM*

MS
G20.5
WAS

Nanotechnology
Nanoparticles
X-Ray diffraction


**Synthesis and Characterization of NiFe₂O₄ nanoparticles by
wet chemical sol-gel method**

By:

Waqas Shoukat

(289-FBAS/MSPHY/F14)

**This Thesis is submitted to the Department of Physics International Islamic University,
Islamabad for the award of degree of
MS Physics Degree**


Chairman, Department of Physics
International Islamic University, Islamabad

*CHAIRMAN
DEPT. OF PHYSICS
International Islamic University
Islamabad*


Dean Faculty of Basic and Applied Science
International Islamic University, Islamabad

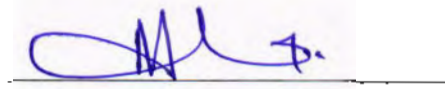
Department of Physics
Faculty of Basic and Applied Sciences
International Islamic University, Islamabad

Final Approval

It is certified that the work presented in this thesis titled “**Synthesis and characterization of Ni Fe₂O₄ by wet chemical solgel method**” by **Waqas Shoukat** (Reg. No.289-FBAS/MSPHY/F-14) fulfills the requirement for the award of degree of MS Physics from Department of Physics, International Islamic University Islamabad, Pakistan.

Viva Voce Committee

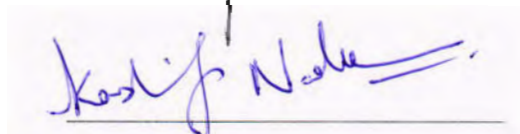
Chairman (Prof. Dr. Mushtaq Ahmed)
(Department of Physics)



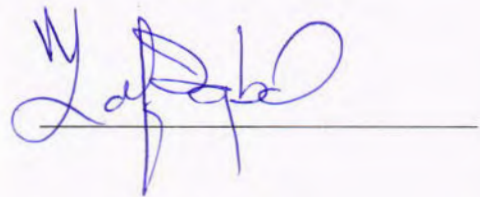
Supervisor (Dr. Syed Salman Hussain)



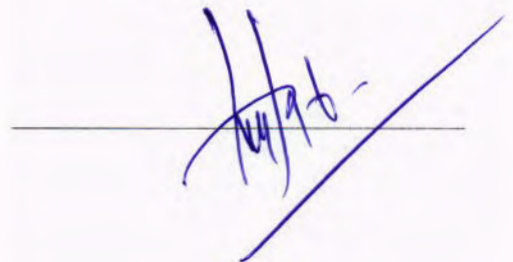
Co. Supervisor (Dr. Kashif Nadeem)



External Examiner (Prof. Dr. Zafar Iqbal)



Internal Examiner (Dr. M. Mumtaz)

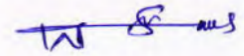




DEDICATED
To
My beloved
Parents
And
My
Respected Teachers

Declaration

I, Waqas Shoukat(Registration # 289-FBAS/MSPHY/F14), student of MS in Physics (session 2014-2016), hereby declare that the matter printed in the thesis titled “ Synthesis and characterization of NiFe₂O₄ nanoparticles by wet chemical sol-gel method” is my own work and has not been published or submitted as research work or thesis in any form in any other university or institute in Pakistan or aboard.



Waqas shoukat

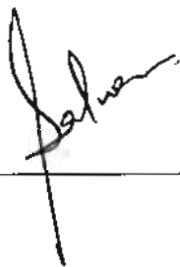
(289-FBAS/MSPHY/F14)

Dated:

FORWARDING SHEET BY RESEARCH SUPERVISOR

The thesis entitled “**Synthesis and characterization of NiFe₂O₄ nanoparticles by wet chemical sol-gel method**” submitted by **Waqas shoukat** in partial fulfillment of M.S. degree in Physics has been completed under my guidance and supervision. I am satisfied with the quality of student’s research work and allow him to submit this thesis for further process to graduate with Master of Science degree from Department of Physics, as per IIU rules and regulations.

Dated: _____



Supervisor

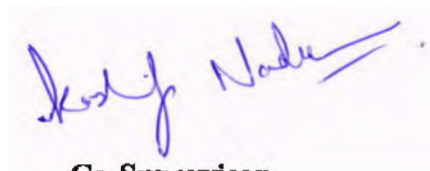
Dr. Syed Salman Hussain

Assistant Professor (TTS)

Department of Physics,

International Islamic University,

Islamabad.



Co-Supervisor

Dr. Kashif Nadeem

Assistant Professor (TTS)

Department of Physics,

International Islamic University,

Islamabad.

ACKNOWLEDGMENT

First, I owe my deepest gratitude to Almighty **Allah** for all of his countless blessings. I offer my humblest words of thanks to HIS most noble messenger **Hazrat Muhammad (P.B.U.H)**, who is forever, a torch of guidance and knowledge for all humanity. By virtue of his blessings today I am able to carry out our research work and present it.

I would like to acknowledge the worth mentioning supervision of **Dr. Syed Salman Hussain** and co-supervision of **Dr. Kashif Nadeem** who guided me and supported me during my whole research work. Their supervision from the preliminary to the concluding level enabled me to develop an understanding of the field. Their wide and deep knowledge have been a great value for me. Frankly speaking without effort of **Dr. Kashif Nadeem** and **Dr. Syed Salman Hussain** it was impossible to complete this hard task of my life. They always enlightened me and guided me at each and every step of my MS. Almighty **Allah** blessed them in every part of life.

Moreover, I would like to express my sincere thanks to all the faculty members of Department of Physics IIU Islamabad especially to Dr. Mushtaq Ahmed (Chairman). I express my thanks to all staff of Physics Department, IIU, for their various services. I also pay special thanks to Dr. Iftikhar Gul and his students Muhammad Zarar and Anum Rubab for providing me opportunity for dielectric in time. I also pay special thanks to Dr. Waqar Adil Syed for providing me opportunity to use FTIR in time. I shall express my heartiest thanks to all my senior research colleagues Faisal Zeb, Muhammad Kamran, Waqas Ali and Liaqat Ali being very supportive and co-operative all throughout my research work. I also pay special thanks to my class fellow Yasir Mehmood Khan, Muhammad Rehan, Rashid ali, ranatoqeerahmed and most especially to Fahad Ali Shah, without their guidance it would have been very difficult to complete this work.

I especially want to acknowledge my father Mr Shoukat Ali, my mother, my elder brother Sajjad Shoukat and my younger brother Bilal Shoukat for their encouragement, support and confidence on me. During my education career their personalities remained the role model for me. Finally I am thankful to my parents for their love, care and support in my life, which has been directly encouraging me for my study. My parents' prayers have always been a big support in solving my problems. May Allah bless my parents and family with long life, health and happiness.

Waqas Shoukat

Table of Contents

Introduction to Nanotechnology	1
1.1 Nanoscience.....	1
1.2 Nanotechnology.....	1
1.3 Nanomaterials.....	1
1.3.1 Zero dimensional nanomaterials (0D).....	2
1.3.2 One dimensional nanomaterials (1D).....	2
1.3.3 Two dimension nanomaterials (2D).....	2
1.4 History of nanotechnology	3
1.5 Applications of nanotechnology.....	4
1.5.1 Medicine	4
1.5.2 Foods	4
1.5.3 Electronics	4
1.5.4 Water purification.....	5
1.5.5 Space.....	5
1.6 Magnetism	5
1.6.1 Magnetic moment.....	6
1.6.2 Diamagnetic materials	8
1.6.3 Paramagnetic materials.....	9
1.6.4 Ferromagnetic materials	10
1.6.4.1 Curie temperature	11
1.6.5 Anti-Ferromagnetic materials	12
1.6.5.1 Neel Temperature	12
1.6.6 Ferrimagnetic materials.....	13
1.7 Ferrites	13
1.7.1 Soft Ferrites	14
1.7.2 Hard Ferrites.....	14

1.8	Types of ferrites.....	14
1.9	Spinal ferrites	15
1.9.1	Classification of spinal Ferrites.....	16
1.9.1.1	Normal Spinal Ferrites	16
1.9.1.2	Inverse Spinal Ferrites.....	16
1.9.1.3	Mixed Spinal Ferrites	16
1.10	Dielectric materials.....	17
1.11	Polarization.....	17
1.12	Types of Polarization.....	18
1.12.1	Electronic polarization	18
1.12.2	Ionic polarization.....	18
1.12.4	Interfacial polarization	20
1.13	Dielectrics.....	20
1.13.1	Dielectric Constant.....	21
1.13.2	Dielectric loss tangent	22
1.13.3	Real part of dielectric constant.....	22
1.13.4	Imaginary part of dielectric constant.....	23
	Literature review and synthesis	24
2.1	Literature Review	24
	Synthesis and characterization techniques.....	29
3.1	Synthesis of nanomaterials	29
3.1.1	Top down approach	29
3.2.1	Flow chart and explanation	30
3.3	Characterization techniques	32
3.4	X-Ray Diffraction (XRD).....	32
3.4.1	X-rays	32
3.4.2	Production of X-Rays.....	33

3.4.3	Bragg's law.....	33
3.4.4	Measurement of particle size.....	34
3.5	Fourier Transform Infrared Spectroscopy (FTIR)	36
3.5.1	Michelson interferomete.....	36
3.5.2	Beam splitter.....	37
3.6	Transmission Electron Microscopy.....	37
3.6.1	Component of TEM.....	38
3.6.1.1	Electron gun.....	38
3.6.1.2	Condenser lens and condenser aperture	38
3.6.1.3	Objective lens	38
3.6.1.3	Intermediate lens	39
3.6.4.4	Projector lens.....	39
3.6.4.5	Image observation	39
3.6.2	Working principle of TEM.....	39
3.7	Energy Dispersive X-rays Spectroscopy (EDX or EDS).....	40
3.8	LCR Meter.....	40
3.8.1	Handheld LCR meter.....	41
3.8.2	Benchtop LCR meter.....	42
	Results and discussion	43
4.1	X-Ray diffraction (XRD)	43
4.4	Transmission Electron Microscopy (TEM)	49
4.5	Dielectric properties	50
4.5.1	Real part of Dielectric	50
4.5.3	Dielectric loss tangent	53
4.5.4	AC Conductivity.....	55
	Conclusions.....	58

List of Figures

Fig. 1.1: Nanotechnology's applications	1
Fig. 1.2: Quantum dots	2
Fig. 1.3: Nanowires.....	2
Fig. 1.4: Thin film.....	3
Fig. 1.5: Magnetic dipole moment.....	7
Fig. 1.6: (a) Orbital magnetic moment and (b) Spin magnetic moment.....	7
Fig. 1.7: Periodic table of magnetic elements.....	8
Fig. 1.8: Diamagnetism.....	8
Fig. 1.9: (a) Graph of magnetic diamagnetic susceptibility with magnetic field (b) with temperature.....	9
Fig. 1.10: Paramagnetism.	9
Fig. 1.11: (a) Graph of paramagnetic susceptibility with magnetic field (b) with temperature.	10
Fig. 1.12: Ferromagnetism.....	11
Fig. 1.13: Temperature's effect on the magnetic materials.	11
Fig. 1.14: Temperature and magnetic response of antiferromagnetic material.....	12
Fig. 1.15: Ferrimagnetic material.	13
Fig. 1.16: Unit cell structure of Spinal ferrites.....	15
Fig. 1.17: (a) Polar molecules in the absence of field (b) in the presence of field.....	18
Fig 1.18 Electronic polarization.....	18
Fig 1.19: Ionic polarization polarization.	19
Fig. 1.20: (a) Without field (b) with field.....	19
Fig. 1.21: (a)In the absence of field(b) in the presence of field.	20
Fig. 1.22: Dielectric between the plates of capacitor.	20
Fig. 1.23: Dielectric tangent loss	22
Fig. 3.1: Electromagnetic spectrum	32
Fig. 3.2: Mechanism of X-rays production.....	33
Fig. 3.3: Diffraction of Rays from the plans of crystal.....	34

Fig. 3.4: FWHM.....	35
Fig. 3.5: Fourier transform infrared spectroscopy (FTIR).....	36
Fig. 3.6: Experimental arrangement of Michelson interferometer	37
Fig. 3.7: (a) Working principle of TEM (b) Transmission Electron Microscope	39
Fig. 3.8: (a) Energy dispersive (b) X-rays Spectroscopy	40
Fig. 3.9: (a) LRC meter 6440B (b) Circuit diagram of bridge of LCR meter	41
Fig. 4.1: XDR pattern of $\text{NiCr}_x\text{Fe}_{2-x}\text{O}_4$ for $x=0, 0.2, 0.4, 0.6, 0.8$ and 2	44
Fig. 4.2: (a) Crystallite size of $\text{NiCr}_x\text{Fe}_{2-x}\text{O}_4$ (b) Lattice constant of $\text{NiCr}_x\text{Fe}_{2-x}\text{O}_4$	45
Fig. 4.3: (a) FTIR spectra of $\text{NiCr}_x\text{Fe}_{2-x}\text{O}_4$	47
Fig. 4.4: EDX of NiFe_2O_4 nanoparticles.....	48
Fig. 4.5: Mapping images of NiFe_2O_4 nanoparticles	49
Fig. 4.6: TEM image of $\text{NiCr}_x\text{Fe}_{2-x}\text{O}_4$ ($x=2$) nanoparticles	49
Fig. 4.7: (a) Real part of Dielectric of NiFe_2O_4	51
Fig. 4.8: (b) Real part of Dielectric of $\text{NiCr}_x\text{Fe}_{2-x}\text{O}_4$ nanoparticles.....	51
Fig. 4.9: (a) Imaginary part of Dielectric of NiFe_2O_4	52
Fig. 4.10: (b) Imaginary part of Dielectric of $\text{NiCr}_x\text{Fe}_{2-x}\text{O}_4$ nanoparticles.....	53
Fig. 4.11: (a) Tangent loss of NiFe_2O_4	54
Fig. 4.12: (b) Tangent loss of $\text{NiCr}_2\text{Fe}_{2-x}\text{O}_4$ for ($x=0.0, 0.2, 0.4, 0.6, 0.8$ and 2).....	55
Fig. 4.13: (a) AC conductivity of NiFe_2O_4	56
Fig. 4.14: (b) AC conductivity of $\text{NiCr}_x\text{Fe}_{2-x}\text{O}_4$	57

Abstract

The nickel ferrites nanoparticles doped with chromium ions on octahedral were synthesized by using conventional sol-gel method. Structural and dielectric properties of $\text{NiCr}_x\text{Fe}_{2-x}\text{O}_4$ nanoparticles have been discussed in detail. X-ray diffraction (XRD) analysis confirmed the cubic inverse spinel structure of the samples with $x = 0, 0.2, 0.4, 0.8, 2.0$ concentration. It was found that, the average crystallite size and lattice constant decreases with increase of Cr^{+3} concentrations. This reduction is most expectedly due to smaller ionic radius of Cr (0.064 nm) as compared to Fe (0.067 nm). EDX analysis was used to confirm elemental composition of our samples shows no prominent presences of other impurities. With the help of TEM analysis shows the hexagonal shape of nanoparticles. Dielectric properties have been explained by using Koop's and Maxwell-Wagner models. Dielectric properties of sample also show dependence on the Cr^{+3} concentrations. Real and imaginary part of dielectric and loss tangent decreased with increasing the frequency and becomes constant in higher frequency area. However, AC conductivity shows an opposite trend and has large values at higher frequencies. This study confirmed the strong influence of Cr^{+3} concentration on the structural and dielectric properties of NiFe_2O_4 nanoparticles.

Introduction to Nanotechnology

1.1 Nanoscience

The branch of science in which the novel characteristics of various materials are studied at nanoscale is known as nanoscience. In this branch, the particles of given material have at least one dimension lies in the range between 1 nm to 100 nm. At this scale, the properties of numerous materials drastically changed as compared to their bulk counterpart [1].

1.2 Nanotechnology

The term nanotechnology is conventionally defined as the practical application of nanoscale materials in manufacturing of various industrial based applications. Quality, performance and strength of nanomaterials is much better than bulk materials. The most expected reason for this increase is larger surface to volume ratio as the size of given material reduce to nanoscale [2].



Fig.1.1: Nanotechnology's applications[3].

1.3 Nanomaterials

The materials have at least one scale in nanometer are termed as nanomaterials. In other words, nanomaterials can be distinguished as, the materials in which from all three lengths at least one can be characterized by the nanometer. Nanoparticles are so small that they have the diameter 10,000 times smaller as compared to the human hair. The nanomaterials have very different properties as compare to bulk conventional form[4]. For example, the bulk gold cannot be used as a catalyst while the gold

nanoparticles exhibit excellent catalytic properties. There are several types of nanomaterials which are given below.

1.3.1 Zero dimensional nanomaterials (0D)

The materials that have all dimension less than 100 nm are called zero dimensional nanomaterials. Examples are nanodots, nanoclusters, nanoparticles, quantum dots etc[5].

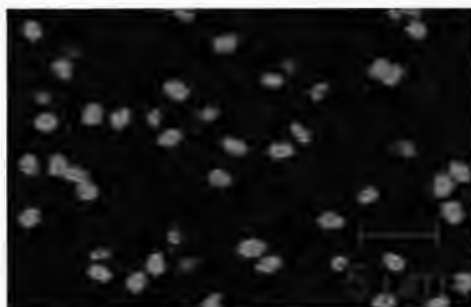


Figure 1.2: Quantum dots[6].

1.3.2 One dimensional nanomaterials(1D)

The materials that have two dimensions in nanoscale. Examples are nanotubes , nanowires etc[5].



Fig. 1.3: Nanowires [7].

1.3.3 Two dimension nanomaterials (2D)

The materials that have one dimension at nanoscale i.e one dimension < 100 nm. Examples are thin films and coatings etc[5].

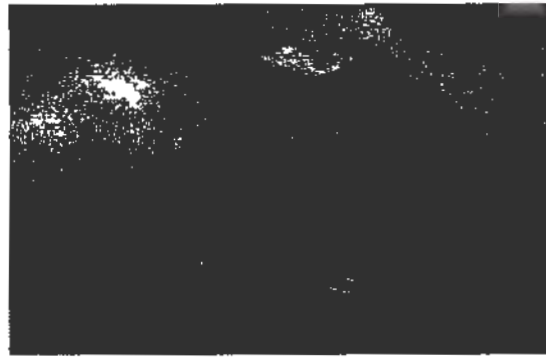


Fig. 1.4: Thin film[8].

1.4 History of nanotechnology

The history of nanomaterials is old but the real revolution in synthesis and characterization using different techniques including XRD, VSM, SEM, TEM etc started after 1959. Now we are capable to design and manufacture devices by moving every atom individually N Taniguchi first time used the word “nanotechnology” in his paper on ion sputtering machining in 1974 [9]. Richard Feynman’s ideas of nanotechnology were built-up by E. Drexler in “Vehicles of creation: the arrival of nanotechnology”, the book written by E. Drexler published in 1986 [10]. Atomic force microscope (AFM) was also invented in 1986[11]. During the period of 1980 to 1990 there is many studies were performed in the field of nanotechnology and number of ways were adopted to promote this branch of physics. In 1991 (CNT’S) carbon nanotubes were synthesized[12]. In 2001 USA took a serious step in the form of National Nanotechnological Initiative(NNI). The objective of this initiative was to show the interest in improvement and development of this technology in Federal Government. In 1996-1998 an exclusive action appeared to support NNI as special committee of American Central for Global Technology Assessment (ACGTA), which organized and promoted the values of nanotechnology all over the world. Mean while Interagency working group on nanoscience (IWGN) back up by Presidential Council on Science and Technology (PCAST) and also NNI got official approval in the year 2000. After that president Clinton granted 500 million dollars to NNI for its development and benefits of nanotechnology.. First time the principal laws and techniques were introduced in industrial field in 1997 by the company “zyves” and created the products of nanotechnology.

In 2000 Government of Japan set a specific department of nanotechnology. In this period lots of countries including Germany, England, France, China, South Korea etc started work on the development of nanotechnology. In 2010 DNA based program assembly started. In 2011 nanoprocessor's circuit was developed.

1.5 Applications of nanotechnology

There are many applications of nanotechnology in our daily life; some of them are given below.

1.5.1 Medicine

The field of medicine is expected to benefit majorly from the field of nanotechnology. Nanoparticles are used for the drug delivery. Nano-engineered drugs can reduce the consumption of drug while increasing its efficiency as well. Nanoparticles can be tuned to accumulate at the site of damage allowing direct treatment of the damaged part. Nanoparticles are being developed to destroy various viruses also[13].

1.5.2 Foods

Researchers are working on the nanomaterials which can enhance the shelf life of food as well as to keep it better for the health. Nanotechnology is being used in the food science from growing of the fruits to the packing of the foods. Silver nanoparticles are being used in the storage bins to destroy bacteria from the foods in the bins and to minimize the harmful effect of the bacteria. In the plastic packaging, the zinc oxide nanoparticles can be used to block the ultraviolet rays and provide the protection from the bacteria and improve the stability and strength of the plastic film [13].

1.5.3 Electronics

Nanotechnology envisions developing the devices of very small size, very large capability and best performance with lower power consumption. In electronics, by using the nanomaterials instead of bulk materials we can reduce the size of electronic devices and enhance the capacity. In future we shall be able to have power of all the computers in the palm of our hand. Data transmission has benefitted a lot by

nanotechnology in which by using silicon nanophotonic component in CMOS circuit, higher speed can be achieved[13].

1.5.4 Water purification

Study has been started for the purification of water through nanotechnology. Industrial wastage is one of the challenges in the purification of water. Harmful chemical can be converted to harmless either by the chemical reaction with the nanoparticles or by using nanoparticles as catalysts. Metal and salt removal is also another challenge. We can convert the salt water to drinking water by using the deionizing method, in which we use electrodes which are made up of nanosize fiber that shows a pledge for reducing the energy and cost for the purification of water [13]

1.5.5 Space

If we talk about the space journey and research, then our main problem is to move the lighter craft, which will reduce the consumption of energy (fuels) provided by rockets, so it will be the low cost approach to desired orbits. This can be achieved by using a low density material with high structural strength which can easily be achieved by embedding nanoparticles on the surface of the material to reduce the wear and tear or by employing grapheme in carbon fibers or other materials[13].

1.6 Magnetism

Many recent technologies such as computers, electric generators, transformer, electric motors and telephone etc. depend upon the magnetic properties of the materials. In magnetism we study the response of material due to the applied magnetic field[14]. Magnetism is the intrinsic property of matter.

As we know that

$$B = \mu H \quad (1.1)$$

H is the magnetic field, μ is the permeability of material and B is the flux density.

Also we know that

$$\mu = \mu_0 \mu_r$$

So equation 1 becomes

$$B = \mu_0 \mu_r H \quad (1.2)$$

Now adding and subtracting $\mu_0 H$ on the right hand side of the equation (1.2)

$$B = \mu_0 \mu_r H + \mu_0 H - \mu_0 H$$

$$B = \mu_0 H + \mu_0 H (\mu_r - 1)$$

$$B = \mu_0 H + \mu_0 M \quad (1.3)$$

Where M is magnetization and $M = H (\mu_r - 1)$

$$\text{As} \quad \chi_m = \mu_r - 1$$

So M can be written as

$$M = \chi_m H \quad (1.4)$$

Where χ_m is the magnetic susceptibility

1.6.1 Magnetic moment

Magnetic dipole moment or magnetic moment is the measurement of the tendency of a material to align in the direction of external magnetic field. Magnetic moment is denoted by "A" and its magnitude is given as

$$M = I * A \quad (1.5)$$

Where I is the current and A is the area of loop. Magnetic moment is a vector quantity. The unit of magnetic moment is $A \cdot m^2$.

There are two main sources of magnetic moment which are spin motion and orbital motion of electrons in the atom. The magnetic moment due to orbital motion of electron is called orbital magnetic moment and it can be considered as the current loop that produces magnetic field and due to this action magnetic moment is created. Another

reason of the magnetic moment is the electron's spin motion. The magnetic moment due to spin motion is called spin magnetic moment. Bohr magnetron is used to express the size of magnetic moment. μ_B is the notation of bohr magnetron. The value of μ_B is $9.3 \times 10^{-24} \text{ A}\cdot\text{m}^2$

The spin magnetic moment in case of electron spin is $\pm \mu_B$, where positive and negative shows up and down spin respectively. $M_j \mu_B$ is the magnetic moment in case of orbital motion. Here m_j is a magnetic quantum number.

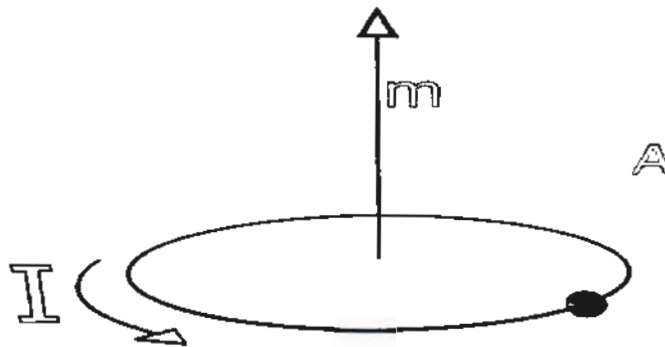


Fig. 1.5: Magnetic dipole moment.

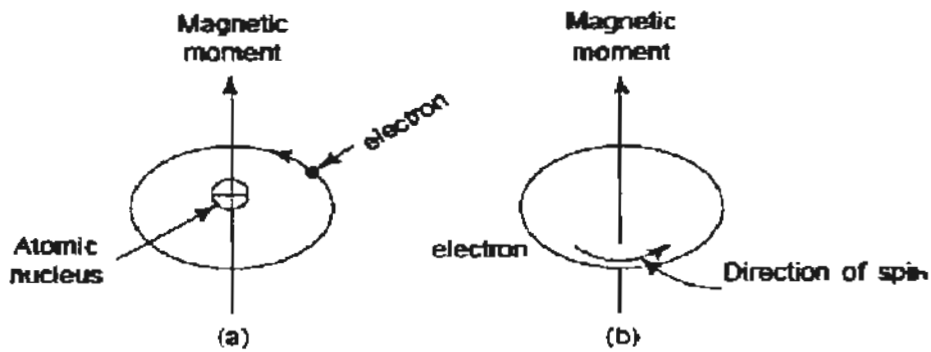


Fig. 1.6: (a) Orbital magnetic moment and (b) Spin magnetic moment.

On the basis of the arrangement of atoms/molecules we can classify the magnetic materials into different types which are given below.

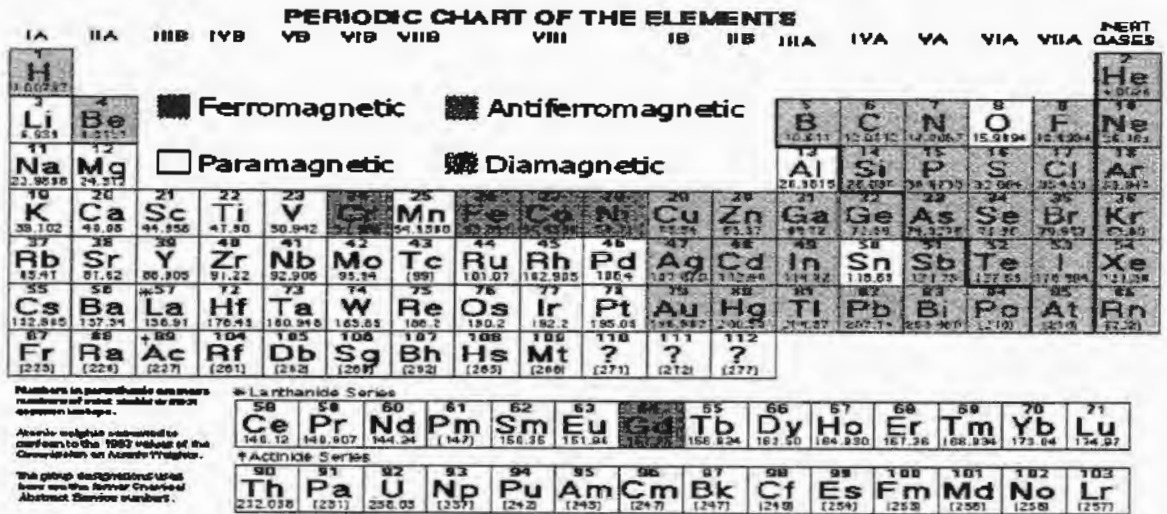


Fig. 1.7: Magnetic behaviors of elements[15].

1.6.2 Diamagnetic materials

These are the materials in which all electronic shells are filled and there is no unpaired electron that can take part in magnetization. Therefore the magnetization is zero. All types of materials have some degree of diamagnetism but have weak effect. In 1847 Michael Faraday first time observed the diamagnetic effect by bringing the bismuth sample near the magnet. Bi, Cu, Ag, Au, Ge, etc are the examples of diamagnetic materials.

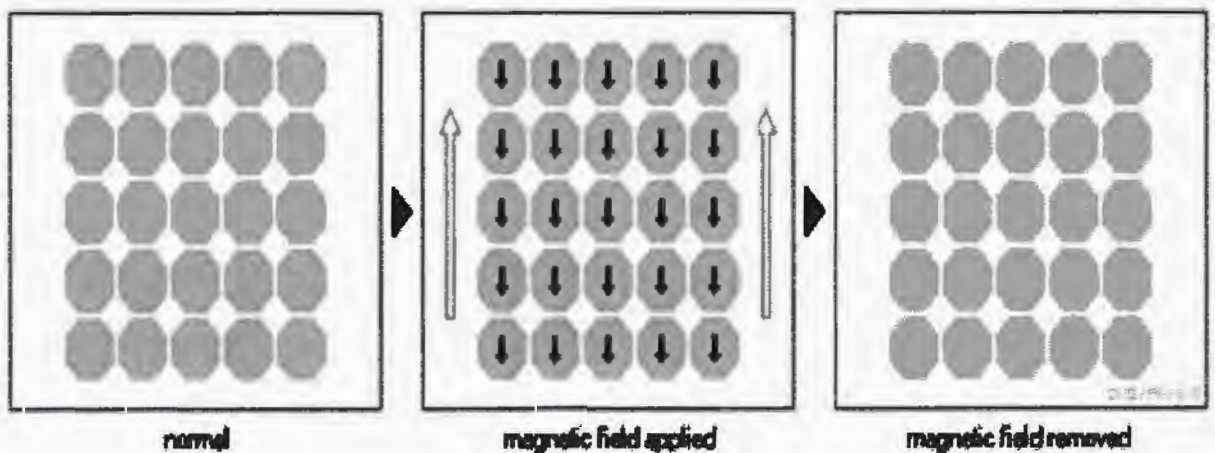


Fig. 1.8: Diamagnetism.

When an external magnetic field is applied the magnetic moments of diamagnetic material align themselves in such a way that they oppose the external magnetic field. Therefore their magnetic susceptibility is negative. As the magnetic moments are caused by external magnetic field so by Lenz's law these magnetic moment will oppose the applied magnetic field. There is no effect on magnetic susceptibility due to change of temperature[14].

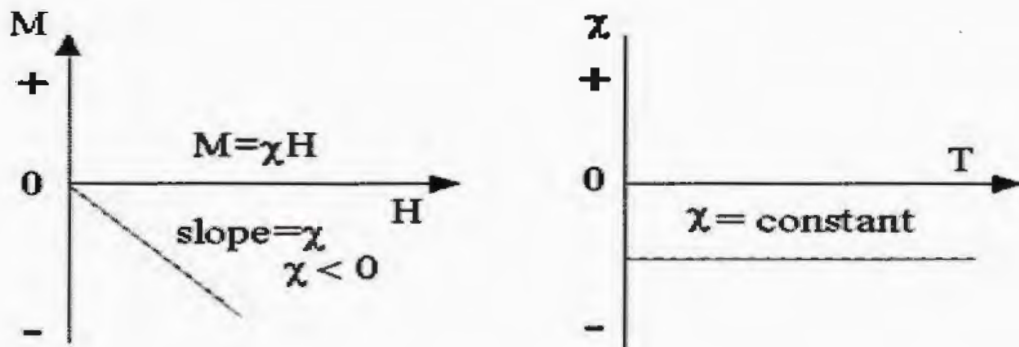


Fig. 1.9: (a) Graph of magnetic susceptibility with magnetic field (b) with temperature.

1.6.3 Paramagnetic materials

These materials having incomplete shells so have unpaired electrons. Therefore they have the magnetic moment related to atoms, but as they are arranged randomly, therefore net magnetization is zero in the absence of external magnetic field. Moreover when external field is applied, arrangement become such that there is net magnetic field so behave like a temporary magnet. Here magnetism depends on the external magnetic field.

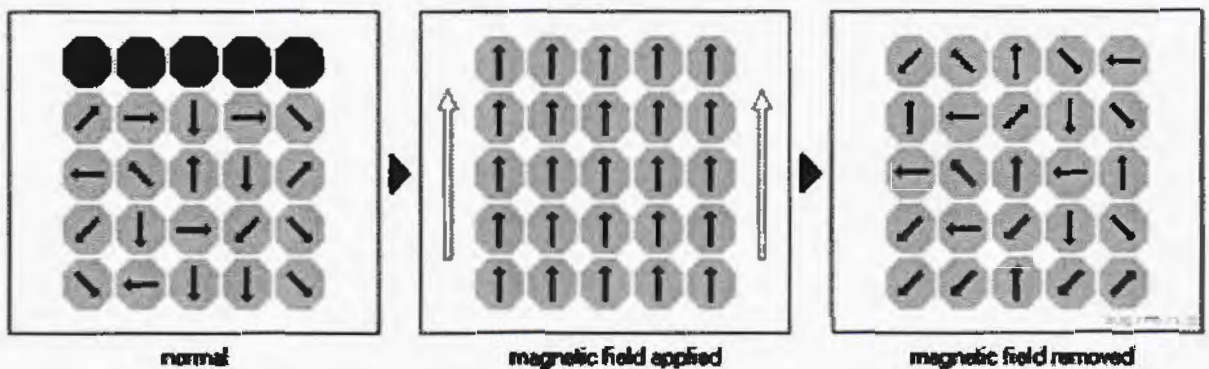


Fig. 1.10: Paramagnetism.

In paramagnetism temperature variation is also effective. Magnetic susceptibility has inverse relation with temperature. When we increase the temperature than randomness of magnetic moments also increases. Therefore magnetic susceptibility is inversely proportion to the temperature. In paramagnetic materials the magnetic susceptibility is positive. Moreover magnetic susceptibility is directly related to applied magnetic field i.e the susceptibility will increase by increasing the magnetic field[14].

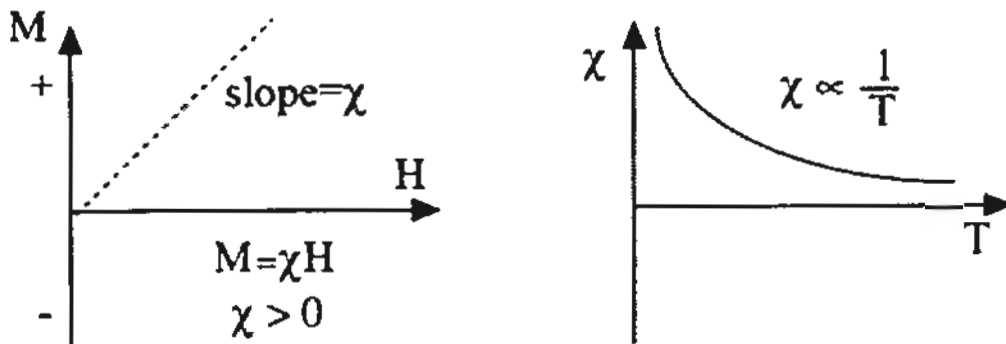


Fig. 1.11: (a) Graph of magnetic susceptibility with magnetic field (b) with temperature.

1.6.4 Ferromagnetic materials

These materials have large number of unpaired electrons and they have magnetic moments which are arranged in a specific direction although there is no magnetic field, mean they have spontaneous magnetization [16]. In ferromagnetic materials there are large amount of domains. Atoms present in each domain are nearly 10^{15} - 10^{16} , so the arranged atom in the domain possesses a strong magnetic field. The transition region which is called domain walls has the thickness of about 100 atoms. In ferromagnetic materials exchange also exist between the magnetic moment. When external field is introduced then magnetic moments arranged themselves in this way that they support the applied magnetic field and behave like a strong magnet. In ferromagnetic materials magnetism remains after the removal of external magnetic field.

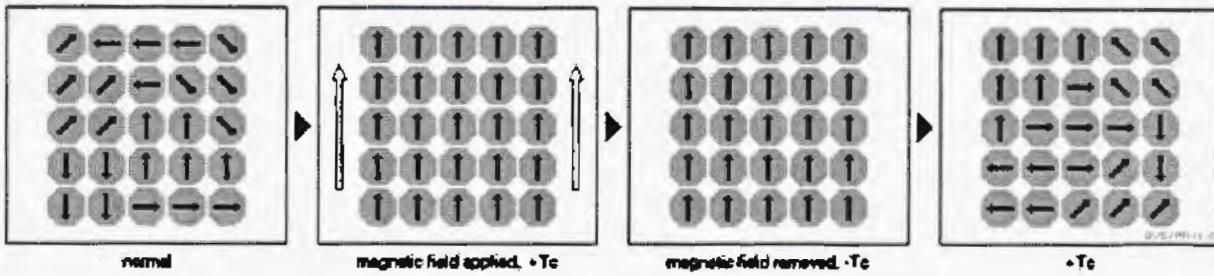


Fig. 1.12: Ferromagnetism.

1.6.4.1 Curie temperature

It is the temperature above which ferromagnetism of some metals like cobalt, nickel and iron dispersed and they tend to become paramagnetic. It was named after Pierre Curie who discovered it. T_c is the notation for curie temperature. According to Curie law

$$\chi = C/(T - T_c) \tag{1.6}$$

χ and T_c are magnetic susceptibility and curie constant respectively.

In ferromagnetic materials below the Curie temperature there is strong interaction but above this temperature randomness of the domains increases because thermal energy reduces the exchange interaction.

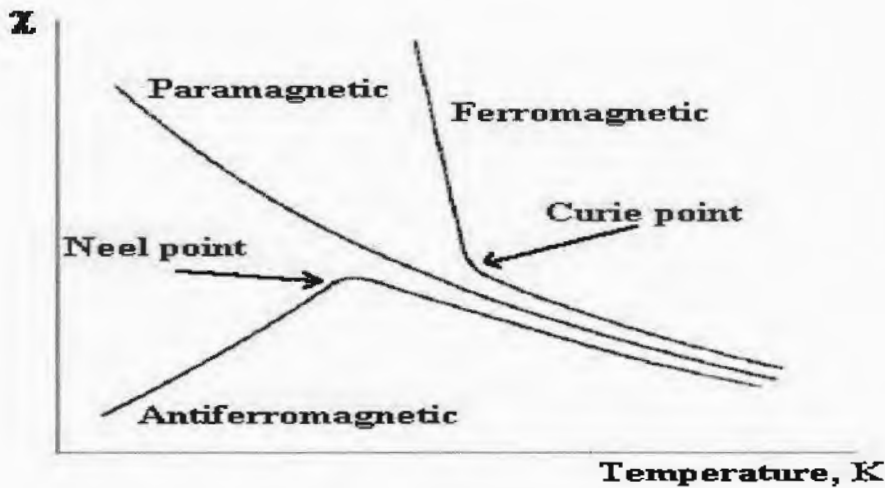


Fig. 1.13: Temperature's effect on the magnetic materials.

1.6.5 Anti-Ferromagnetic materials

These are the materials in which the spin of the neighboring magnetic moment is antiparallel. Those materials have no magnetization due to this unlike parallel arrangement of magnetic moments. In anti-ferromagnetic materials the exchange interaction is negative. Two types of sub-lattices are present in anti-ferromagnetic materials which are responsible for this behavior. One sub-lattice has magnetic moment in upward direction and other has magnetic moment in down ward direction. In the presence of external magnetic field domains align themselves and they show some magnetic behavior. MnO is the material in which anti-ferromagnetism was observed for the first time. There is a temperature above which anti-ferromagnetism of the material vanishes and material tends to become the paramagnetic, that temperature is called Neel temperature[16].

1.6.5.1 Neel Temperature

It is temperature above which anti-ferromagnetic materials loses their anti-ferromagnetism and tend to become the paramagnetic because due to increase in temperature the reduction magnetization phenomenon happens and due to this randomness of the magnetic domains increased. T_N is the notation for neel temperature. We can express the relation between magnetic susceptibility and temperature as given below

$$\chi = C / (T + T_N) \quad (1.7)$$

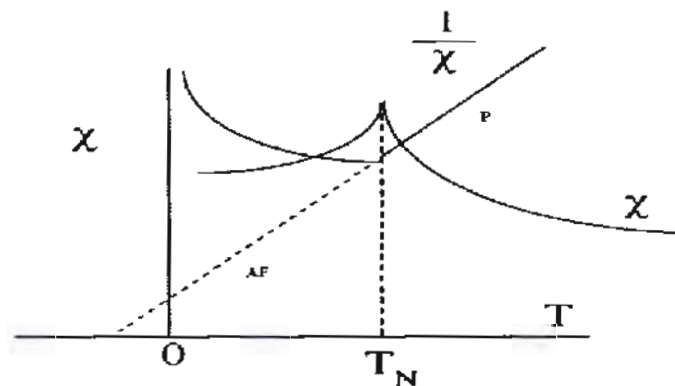


Fig. 1.14: Temperature and magnetic response of antiferromagnetic material.

When we increase the temperature then magnetic susceptibility will increase upto certain maximum value. The temperature at that value of magnetic susceptibility is called neel temperature. Now further increase in temperature decreases the magnetic susceptibility

1.6.6 Ferrimagnetic materials

These are the compound in which magnetic moments are oppositely aligned but are of different magnitudes, so have a net magnetic moment in the absence of external magnetic field. In ferrimagnetic materials there are two sub lattices which are unequal and opposite e.g these sub lattices are A and B, if A sub lattice has dipole moments in the upward direction then B sub lattice will have downward direction. In ionic compound this type of magnetization occurs. Due to the application of external magnetic field these magnetic moments modify their orientation, hence support the magnetic field and increase the magnetization[14].

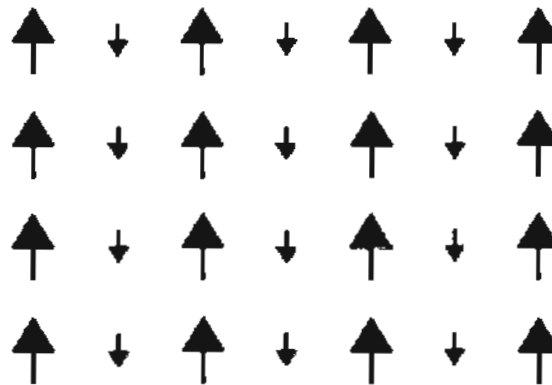


Fig. 1.15: Ferrimagnetic material.

1.7 Ferrites

These are the magnetic materials which have electrical as well as magnetic properties. Ferrites are polycrystalline in nature. Main constituents of ferrites are metal

oxides and iron oxides. General formula of ferrite is XFe_2O_3 , where X is divalent such as Mn^{2+} , Co^{2+} , Ni^{2+} etc[17]. Mankind known the importance of ferrites for many centuries ago, but in 1930 the particular study of their electrical, structural and magnetic properties were started. After that many researchers broadly studied the ferrites. Ferrites have low dielectric and eddy current losses and have high electrical resistivity, high permeability, high saturation magnetization and moderate permittivity. Ferrites are the unique materials which have large applications in various fields. Ferrites can be divided into two classes on the basis of their structure and composition which are given below.

(1) Soft Ferrites

(2) Hard Ferrites

1.7.1 Soft Ferrites

Soft ferrites are those materials that can be magnetize and demagnetize easily. The hysteresis loop of soft ferrite is narrow and these ferrites have lower coercivity. The coercivity of soft ferrites is generally less than 10KA/m. These materials are brittle and chemically inert. Soft ferrites can be used in transformer cores due to low coercivity. If a material have low coercivity then its magnetization can be reverse easily[16]. Spinal and Garnets belongs to soft ferrites.

1.7.2 Hard Ferrites:

Hard ferrites are those materials that are hardly to magnetize and demagnetize. Hard ferrites have high remanence and coercivity. Hard ferrites coercivity is greater than 10KA/m. These are the compound of iron oxide, strontium and barium elements. After the removal of external magnetic field, strength of hard ferrites decreases gradually because of the permanent magnetization in hard ferrites. Hard ferrites can be used in microwave oven magnetron, magnetic door, and load speakers etc. Hard ferrites have very large range of applications in tunable devices, phase shifter and communications devices. The operating temperature of the hard ferrites vary between -40C to 250C depending on the material composition and geometry[16].

1.8 Types of ferrites

On the basis structural properties ferrite can be divided into different classes that are given below.

- Garnets
- Hexagonal ferrites
- Spinal ferrites

But I am interested in the study of spinal ferrites because my sample nickel ferrites have spinal structure.

1.9 Spinal ferrites

General formula of spinal ferrites is AB_2O_4 where A is tetrahedral and B is octahedral and O is oxygen anion site. B is Fe and is trivalent and A is divalent ion such as Mg, Zn, Co, Ni etc. Spinal ferrites have cubic unit cell and have 32 oxygen ions. Spinal ferrites have FCC structure. Spinal ferrites have low resistivity and have small eddy current [18]. In 1915 Nishikawa and Bragg discover spinal ferrites. Spinal ferrites generally have low magnetic anisotropy and they are soft ferrites in nature i.e they have low coercivity. But in some cases they can have large coercivity as well as strongly magnetic anisotropic. When spinal ferrites placed in the varying magnetic field, their hysteresis loop is same like as ferromagnetic materials. Following figure show the spinal structure.

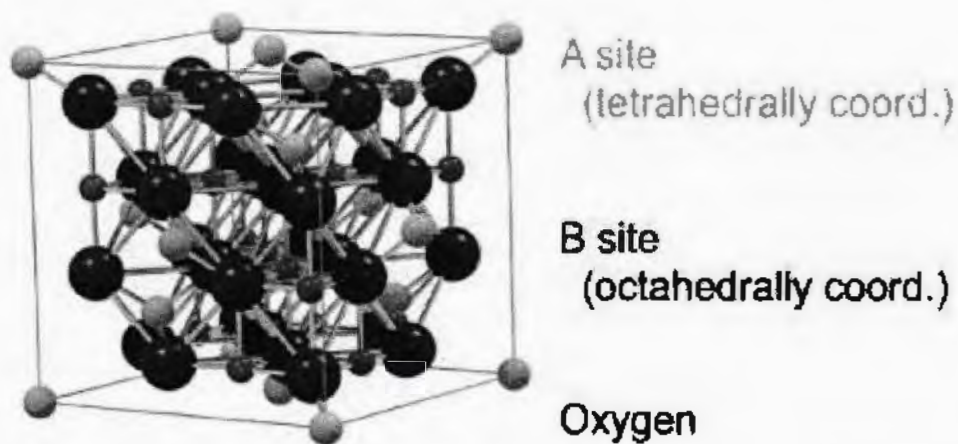


Fig. 1.16: Unit cell structure of Spinel ferrites.

1.9.1 Classification of spinel Ferrites

On the basis of cat-ions distribution there are three classes of spinal ferrites that depends on order of A and B and kind of ions, these types are given below.

Normal spinal ferrites

Inverse spinal ferrites

Mixed spinal ferrites

1.9.1.1 Normal Spinel Ferrites

General formula of normal spinel ferrites is AB_2O_4 . At tetrahedral site A all the ions are divalent and at octahedral B are trivalent. There are 64 tetrahedral sites in which 8 are filled and 32 octahedral sites in which 16 are filled. The octahedral sites are larger than tetrahedral sites. An example of normal ferrites is Mineral spinel $ZnFe_2O_4$ [19].

1.9.1.2 Inverse Spinel Ferrites

Inverse spinel structures have an unusual cat-ion distribution. Here half of the octahedral (B^{3+}) cat-ions occupy octahedral site while other half occupy tetrahedral site and tetrahedral cations (A^{2+}) occupy octahedral site. An example is Fe_3O_4 , if the Fe^{2+} (A^{2+}) ions are d^6 high-spin and the Fe^{3+} (B^{3+}) ions are d^5 high-spin [19].

1.9.1.3 Mixed Spinel Ferrites

Mixed spinel ferrite is an intermediate case where tetrahedral sites and octahedral sites mixed with each other. Their distribution can be described as $(A_{1-x}B_x)[A_{x/2}B_{1-x/2}]_2O_4$, where brackets $[\]$ and parentheses $()$ are used to indicate octahedral sites tetrahedral sites respectively.

Mixed spinals ferrites are pretty and nice means of increasing the magnetic moment. As we know that magnetic moments of tetrahedral and octahedral sites are antiparallel, so falling the magnetic moment of one site will increase the total magnetic moment.

Therefore mixing of normal spinel (ZnFe_2O_4) and inverse spinel (NiFe_2O_4) results in maximization of moment up to ~40 mol% ZnFe_2O_4 [20].

1.10 Dielectric materials

There are three types of materials that are conductor, semiconductor and insulators. In conductors there are free electrons in the materials. In conductors conduction band and valence band are overlapping so free electrons in the valence band can easily move to the conduction band so current can flow easily and there is very low resistance. In semiconductors conduction band and valence band are not overlapped but are close to each other, so by forcing valence electrons to jump to the conduction band. Now the last one are insulators, in insulators the valence band and conduction band are so far, so electrons cannot jump from valence band to conduction band. In insulators the conduction band is totally empty and the valence band is totally filled. Basically insulators are the dielectric materials. When external magnetic field is applied to these materials then they polarize. Due to resistance of insulators these materials are used in electrical circuits.

The behavior of ferrites is just like the insulators. They have large resistance and due to their behavior they are stable. As ferrites are hard in nature and chemically strong so they are very important materials[21]. They can be produced by different methods and exist in different size ranges.

1.11 Polarization

Polarization can be defined as dipole moment per unit volume. Mathematically it can be written as

$$P = \sum p/v \quad (1.8)$$

In dielectric materials the negative charges (electrons) or positive charges (nucleus) would not take the measurable motion in the existence of external field (electric), but set themselves in the stable way. This is known as polarization and the stressed dielectric material is called polarized. The rotation and stretching are the two ways by which

dielectric materials can be polarized. Interfacial interaction and dipole interaction are the reasons for polarizations [22]. In the absence of external electric field polar molecules are randomly align, in the presence of external electric field polar molecules align themselves in the direction of electric field.

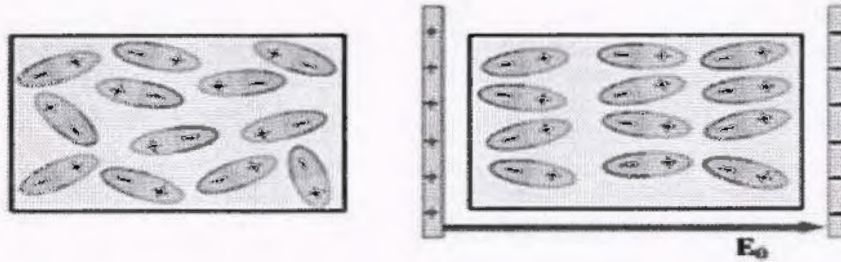


Fig. 1.17: (a) Polar molecules in the absence of field (b) in the presence of field[23].

1.12 Types of Polarization

There are four basic types of polarization which are given below

1.12.1 Electronic polarization

Electronic polarization is also called atomic polarization. In dielectric materials the electrons are restricted to a particular nucleus and the atom is neutral. So it can be imagined that there is no effect of magnetic field on that atom but also we know that every atom has positive charges (nucleus) as well as negative charges (electrons) so the nucleus will shifted toward the negative plate of the electric field and electron cloud will shifted toward the positive plate, therefore atom will ionized due to the external electric field

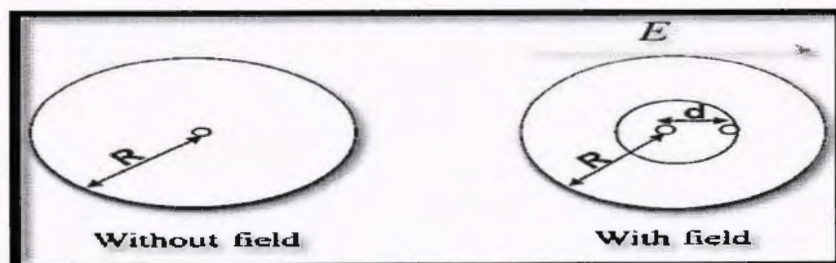


Fig. 1.18: Electronic polarization.

1.12.2 Ionic polarization

This type of polarization occurs in those materials that have ionic character. When field is applied then positive charges align in the direction of field and negative charges align opposite to it, resulting in the formation of dipole moment. Example of ionic material is NaCl.

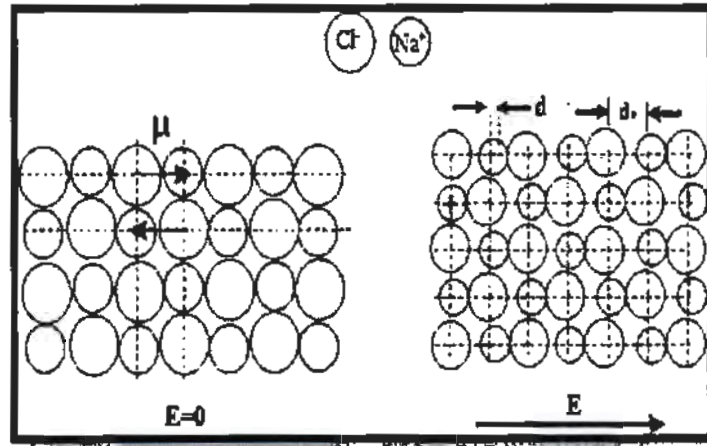


Fig 1.19: Ionic polarization

1.12.3 Orientation polarization

It occurs in the materials which have natural dipole moment. When external field is applied then this field aligns that's dipole in specific orientation. In orientation magnetization, orientation changing all the time because of molecules motion. The perfect example of orientation polarization is water (H₂O) in liquid form [24].

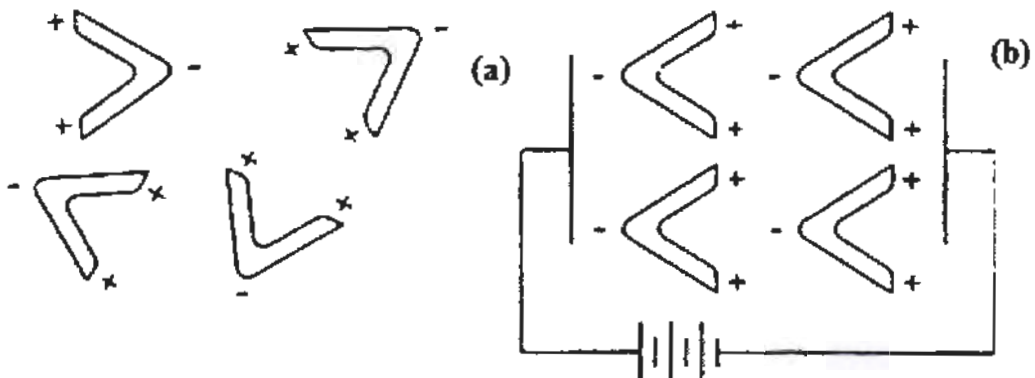


Fig. 1.20: (a) Without field (b) with field.

1.12.4 Interfacial polarization

This polarization is also called space charge polarization. This type of polarization occurs in the materials due to diffusion of ions in the direction of applied field. In the absence of field the ions are arranged in the orderly direction but when the field is applied then ions diffused because of this field. Due to this polarization occurs which is called interfacial polarization. This polarization normally occurs in semiconductors and ferrites.

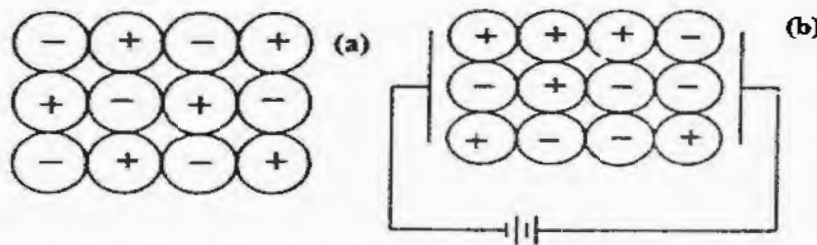


Fig 1.21: (a) In the absence of field (b) in the presence of field.

1.13 Dielectrics

A nonmetallic material between the plates of a capacitor is called dielectric. Without dielectric when voltage is applied across the capacitor's plates it is observed that less charges are stored as compared to the case in which dielectric is introduced between the plates. It means due to dielectric the energy storage is greater than the capacitor with vacuum between the plates [25] .

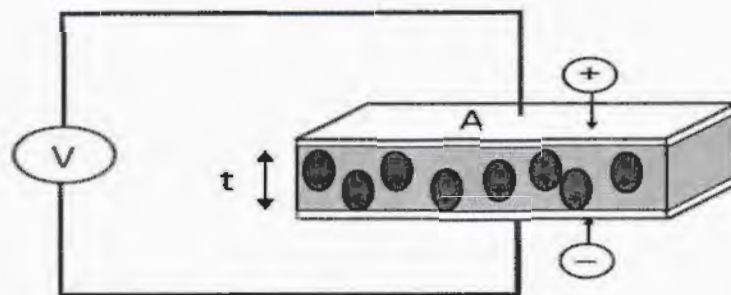


Fig. 1.22: Dielectric between the plates of capacitor.

The capacitance increased due to polarization. We can also say that when a object store the energy in the existence of outer electric field then that object is called dielectric.

1.13.1 Dielectric Constant

It is the property of an insulating material and can be define as ratio of the capacitance of capacitor when insulator medium is placed between the parallel plates to the capacitance of capacitor without medium. It is denoted by κ . If C is the capacitance of capacitor in which dielectric is placed and C_0 is the capacitance of capacitor without medium then mathematically dielectric constant can be written as:

$$\kappa = C/C_0 \quad (1.8)$$

Where κ is the dielectric constant and it is a number and has no dimension.

Dielectric constant is always greater or equal to 1.

For parallel plate capacitor the capacitance can be given as

$$C = \kappa \epsilon_0 A / d$$

Here d is the thickness of the plates; A is the cross sectional area and can be calculated as

$$A = \pi r^2$$

R is the radius of the plates.

From this equation we can say that if the dielectric constant is maximum than capacitance will be maximum. Some time we called the dielectric constant as relative permittivity[25].

Above relation can also be written as

$$\epsilon_r = \epsilon / \epsilon_0 \quad (1.9)$$

Where ϵ_0 is the permittivity of free space and its value is 8.85×10^{-12} F/m

ϵ is the permittivity of the medium.

ϵ_r is the relative permittivity.

Permittivity can be written as

$$\epsilon = D/E \quad (1.10)$$

Where D is displacement vector and E is electric field.

1.13.2 Dielectric loss tangent

As in case of capacitor current lead the voltage by 90° in the absence of any dielectric medium. When we place a dielectric in between the plates, then energy is loss and phase shifted from 90° to $(90^\circ - \delta)$.

Dielectric loss tangent can be defined as the angle between the impedance vector and the negative axis, as shown in diagram.

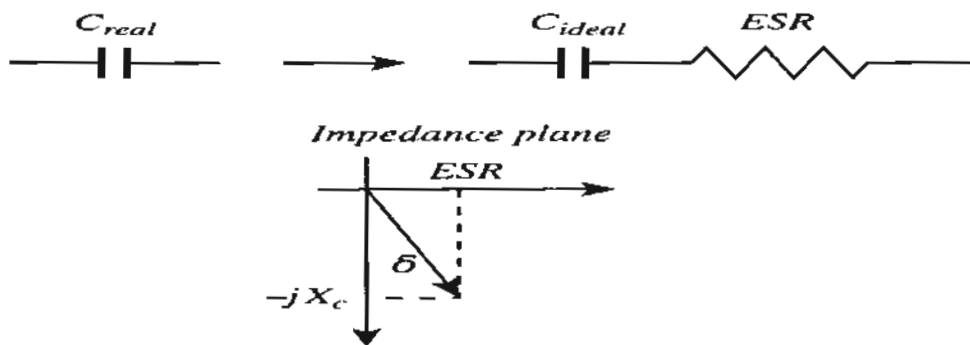


Fig. 1.23: Dielectric tangent loss.

The dissipation factor or loss of energy or tangent loss can be calculated by the relation that is given below:

$$\tan \delta = \sigma / \omega \epsilon$$

$$\tan \delta = 1 / 2\pi f RC \quad (1.11)$$

Here, δ is loss angle, f is the frequency, C is the capacitance and R is the resistance.

1.13.3 Real part of dielectric constant:

Real part of dielectric tells us that how much amount of energy is stored in the material when electric field is applied to the material. Real part of dielectric constant can be express as

$$\epsilon' = C/C_0$$

Where ϵ' is the real part C_0 is the capacitance in the absence of dielectric and C is the capacitance in the presence of dielectric[25]. Real part of dielectric can be calculated by the following equation

$$\epsilon' = (c*d)/(\epsilon_0 * A) \quad (1.12)$$

Where c is the capacitance d is the thickness of pallet of measuring sample ϵ_0 is the permittivity having value $8.85E^{-12}$ and A is the area of pallet.

1.13.4 Imaginary part of dielectric constant

When we apply electric field to the plates of capacitor then dielectric turns into polarized form, as a result charges will start back and forth motion because molecules are displaced. In case of in phase oscillation there is no energy loss. If dielectric molecules collide to each other, as a result energy will be loss in form of heat, this is known as dielectric loss. ϵ_r (Dielectric constant) is the complex No and it is given below:

$$\epsilon_r = \epsilon_r' - j \epsilon_r''$$

here ϵ_r' is the real part of dielectric and ϵ_r'' is the imaginary part of dielectric. The imaginary part can be calculated as:

$$\epsilon_r'' = \epsilon_r' \tan \delta \quad (1.13)$$

Imaginary part of dielectric is the overall amount of energy loose by the material.

Literature review and synthesis

2.1 Literature Review

Barathiraja *et al.*[26]used microwave combustion technique to synthesize $Mn_xNi_{1-x}Fe_2O_4$ nanoparticles (with $x = 0.0-0.5$). The XRD confirmed the single phase spinal structure of nickle ferrites nanoparticles. The crystallite size of samples calculated by scherrer formula lies in range of 11.49 to 17.24 nm. HR-SEM revealed the formation of nanoparticles. The HR-TEM revealed the particles size of nickel ferrites nanoparticles lies between 15 and 20 nm. The EDX verified the elemental composition and showed good agreement with the XRD result. The optical band gap of nickel ferrite nanoparticles were slightly increased by inceasing doping level of Mn as observed by photoluminescence and diffuse reflectance spectra. Optical band gap increased due to finite size effect. The vibrating sample measurements showed a maximum value of saturation magnetization (67.82 emu/g) for $Mn_{0.5}Ni_{0.5}Fe_2O_4$. The doping value of Mn with $x=0.5$ found to have larger surface area than rest of all and shows best catalytic properties.

M.Ishaqueet *al.* [27] synthesized soft ferrites of $Ni_{0.6}Zn_{0.4}Y_{2x}Fe_{2-2x}O_4$ by double sintering ceramic method. Influence of Y^{3+} on electrical, structure, morphology and dielectric properties was studied. For $x \leq 0.06$ the structure of sample was single phase but for $x > 0.06$ there was also small orthorhombic phase peak appeared. Grain growth reduced by doping of yttrium. FTIR spectra confirmed the spinal structure of samples. By increasing the concentration of Y^{3+} it was observed that the dc electrical resistivity increased whereas the dielectric tangent loss and dielectric constant were significantly decreased, so dielectric parameters reduced.

Aleksandar *et al.*[28] synthesized the $NiFe_2O_4$ powder by sub-critical and super-critical situation of ethanol in the reaction. $NiFe_2O_4$ powder obtained by these two methods has primary particles which are similar to particles formed by the co-precipitation method but have higher mesoporosity. They found that magnetic properties directly depend on annealing temperature. The samples provide higher alteration, higher $NiFe_2O_4$ content and higher yield and square shaped hysteresis loop which were prepared

under super-critical situation and also by annealing the average crystallite size became larger. The annealing temperature and time considerably influence magnetic properties such as coercivity and remanance, and also morphology of the required powders.

Aakash *et al.*[29] synthesized $\text{Ni}_{1-x}\text{Mn}_x\text{Fe}_2\text{O}_4$ nanoparticles (with $x=0.05, 0.10, 0.15$) by the co-precipitation method. The prepared particles were of pure spinel phase which was confirmed by XRD and homogeneous particles were formed. In the sample there were cationic vacancies which were confirmed by using GSAS due to refinement of pattern. Strain present in the sample was confirmed by Williamson Hall plot. Mossbauer spectra showed that prepared samples acquired low magnetocrystalline anisotropy coupled and have ferrimagnetic character. Moreover, the Mossbauer spectra investigation confirmed that for Mn ions with low concentration favor to live in tetrahedral sites but for high concentration the spinel became the inverse.

Deng Ni *et al.*[30] synthesized nanocrystallite Ni-Zn ferrites by the method of solvo-thermal. Microstructure and magnetic properties were studied by changing the parameters such as time and temperature of the solvo-thermal reaction and ratio of Zn^{2+} and Ni^{2+} . Particles became homogeneous and bigger by increasing the reaction time. Saturation magnetization gets increased by increasing Ni^{2+} . The saturation magnetization became highest when the concentration was $x=0.30$ and that value is $71.515 \text{ A}\cdot\text{m}^2/\text{kg}$ while the value of saturation magnetization observed to be lowest when concentration reduced to $x=0.20$ and that value is $61.988 \text{ A}\cdot\text{m}^2/\text{kg}$.

Anjum *et al.*[31] prepared the nanoparticles of $\text{Ni}_{1-x}\text{Cu}_x\text{Fe}_2\text{O}_4$ with ($x=0, 0.2, 0.4, 0.6, 0.8$) with the help of double sintering method. The prepared sample was soft ferrites. Lattice parameter increased by doping with Cu because the ionic radius larger than Ni. VSM was used to investigate the magnetic properties. By increasing the concentration of Cu, saturation magnetization was found to be decreased. At high frequency the AC conductivity was increased while dielectric constant was decreased.

Polaert *et al.*[32] used plasma technology for the synthesis of NiFe_2O_4 nanoparticles and studied dielectric properties and magnetic properties at 2.45GHz and temperature ranging from 293 to 513 K in a resonant cavity. The adiabatic heating (no heat enter or leaves the system) of NiFe_2O_4 was modeled under microwave irradiations.

The Maxwell's equations along with the transfer of heat are mathematically solved. The effective parameters are also discussed which includes bed volume, porosity and microwave incident power. At strongest magnetic field energy absorption and conversion into heat is maximized, although the dielectric losses contribute to a smaller degree to the energy conversion and heating. However, the magnetic losses decline with temperatures approaching the Curie temperature and, based on the measured trends, the electric losses increased with temperature. Therefore at higher temperature the contribution of electric losses to heat conversion should increase. By centering the magnetic field over the bed, an efficient and high energy upto 90% is achieved. By proper tuning of cavity the materials bio-functionality become active enough from room temperature to a certain higher temperature, that enhance heat conversion.

Moradmard *et al.*[33] prepared the Mg doped NiFe_2O_4 by the co-precipitation method and annealed at 900°C . XRD revealed that the sample has spinal structure. By increasing the concentration of magnesium it was found that lattice constant and average crystallite size varies. By doping the Mg in NiFe_2O_4 saturation magnetization decreased whereas coercivity increased. Dielectric loss, dielectric constant and ac conductivity of the samples were also studied. It was found that by increasing the frequency dielectric permittivity decreased. Saturation magnetization decreased due to the noncollinearity which was generated due to surface effects and finite sized. As the Fe has smaller ionic radius than Mg so by the replacement, Fe by Mg, coercivity increases. Real part of dielectric decreased whereas imaginary part increased by increasing frequency. At lower frequency range ϵ' achieved higher value. In the intermediate region of frequency there was low variation in dielectric constant.

Joshi *et al.*[34] prepared the nanoparticles of nickel ferrites by the method of co-precipitation. Magnetic, structural and optical properties were investigated by changing the temperature. By varying the sintering temperature, the crystal size varied between the 8nm to 20nm. The ramanance, coercivity and saturation magnetization increased by increasing the sintering temperature. In NiFe_2O_4 , strong surface effects were found at high field. At all the frequencies tangent loss, AC conductivity and dielectric permittivity showed a strong dependence on the sintering temperature. UV spectra showed that there is indirect band gap in the nickel ferrites which is in the range 1.27-

1.47eV. Ni^{2+} occupied both tetrahedral as well as octahedral sites and confirmed the mixed spinel structure.

Ganjali *et al.*[35] prepared the $\text{Ni}_{1-x}\text{Co}_x\text{Mn}_y\text{Fe}_{(2-y)}\text{O}_4$ powder where ($x=y=0.01, 0.02$) by solgel method. By XRD analysis it was concluded that prepared samples were of cubic spinel structure. The effect of calcination temperature on the magnetic and structural properties of samples was determined. By increasing the calcination temperature it was observed that particle size was increased. Scherrer formula was used to determine the nanoparticles size. When the calcination temperature was increased, it was found that saturation magnetization was increased whereas it was also found that coercivity decreased while increasing calcination temperature. At the temperature of 800°C the properties of both the samples were compared.

Gagan dixit *et al.*[36] prepared the nanoparticles of $\text{NiCe}_x\text{Fe}_{2-x}\text{O}_4$ ($x=0.0$ to $x=0.10$). They studied the optical, structural and magnetic properties of these nanoparticles. Except with the concentration $x=0.10$ all the samples have spinel structure. By increasing the concentration of Ce it was found that size of crystal was decreases gradually. By doping with the Ce to pure nickel ferrite, with the FTIR spectroscopy it was found that bands analogous to Fe-o was shifted to the higher wave number. Mossbaures spectra reveal that all the samples were ferromagnetic. By doping with Ce it was also found that saturation magnetization decreased so magnetization reduced whereas magnetic moment's variation was irregular and there was increment in the optical band gap was observed.

Jiao Wan-li *et al.*[37] synthesized nickel ferrites nanopowder by low temperature solid state reaction and then the sample was modified with Ag. They found that silver which has amorphous structure can efficiently stop growing up and reuniting of nanosized nickel ferrites. The nickel ferrites nanoparticles which were modified by 1.5% silver have been sensitivity reaches to 43 for acetone gas, it was 4 times higher than the pure NiFe_2O_4 and doubled as compare to 1.5% mixed nickel ferrites nanoparticles at the voltage of 4.5V. The NiFe_2O_4 nanoparticles which were modified by 1.5% silver were remarkable higher sensitivity to acetone than other gasses. The recovery and response time of such sensor is 10sec and 1 sec respectively.

Sivakumar *et al.*[38] used two polymers of different concentrations for the synthesis of NiFe₂O₄ nanoleaf by conventional sol-gel method. Using sol-gel NiFe₂O₄ nanosheets were synthesized for the first time. Different characterization techniques like HRTEM, TEM, HRSEM, XRD, FTIR, VSM, micro Raman, Dielectric and TGA are used for both nanoleaf and nanoparticles of NiFe₂O₄. XRD and FTIR results verify formation of pure NiFe₂O₄ nanoleaf which completely decomposes at 510° C. The higher concentration of PVA forms nanoleaf. The dielectric constant decreases with the variation in frequency. At room temperature (300° C) the nanostructure exhibits superparamagnetism. The saturation magnetization (M_s) of NiFe₂O₄ NP's and nanoleafs are found to be 46.53 and 44.75 emu respectively. The decrease in value of M_s is due to the high value of PVA and spin effect of small nanoparticles.

Ahmed *et al.*[39] synthesized nickel ferrite nanoparticles by citrate method. XRD pattern shows that the sample has spinel cubic structure. By doping Ag in NiFe₂O₄, it was revealed that the lattice parameter was slightly increased while the Curie temperature decreased by increasing the Ag. By increasing Ag content, the effective magnetic moment and χ_M were decreased. This was expectedly due to the fact that by doping Ag, the distance between cation and anion increased, by which magnetic exchange interaction decreased.

Airimioaei *et al.*[40] prepared Ni_{1-x}Mn_xFe₂O₄ (where x=0, 0.17, 0.34, 0.50) powder by sol-gel method. By increasing the concentration of Mn in nickel ferrite it was observed that saturation magnetization decreased and coercivity increased. Due to the decrease in the saturation magnetization, the particle size reduced. Dielectric properties were measured in the 10 Hz to 1 MHz. By increasing the Mn in nickel ferrites it was observed that dielectric permittivity was increased. By increasing the concentration of Mn, complex impedance representation showed that ceramic ferrites were inhomogeneous. Single impedance arch shown by particles with composition at x=0 and 0.17 and multi impedance arch shown by the particles with composition at x=0.34 and 0.50. Ni_{1-0.17}Mn_{0.17}Fe₂O₄ spinel compound was synthesized by doing several experiments to achieve the best magnetic and structural properties and became the most suitable candidate for chip device applications.

Synthesis and characterization techniques

3.1 Synthesis of nanomaterials

There are two approaches to synthesized nanomaterials. These two approaches are given below.

- Top down approach
- Bottom up approach

3.1.1 Top down approach

In this approach nanomaterial/nanoparticles are synthesized by grinding or breaking down the bulk material to convert it at nanoscale. There are many processes including ball milling, laser ablation, sputtering deposition etc.

3.1.2 Bottom up approach

In this approach the nanoparticles/ nanomaterials are synthesized by gathering the atomic or molecular size particle to convert them into nanosize. That approach includes the process such as electrochemical deposition, co-precipitation, sol-gel process etc. Here nanoparticles was synthesized by sol-gel process which is explained this below

3.2 Sol-gel method

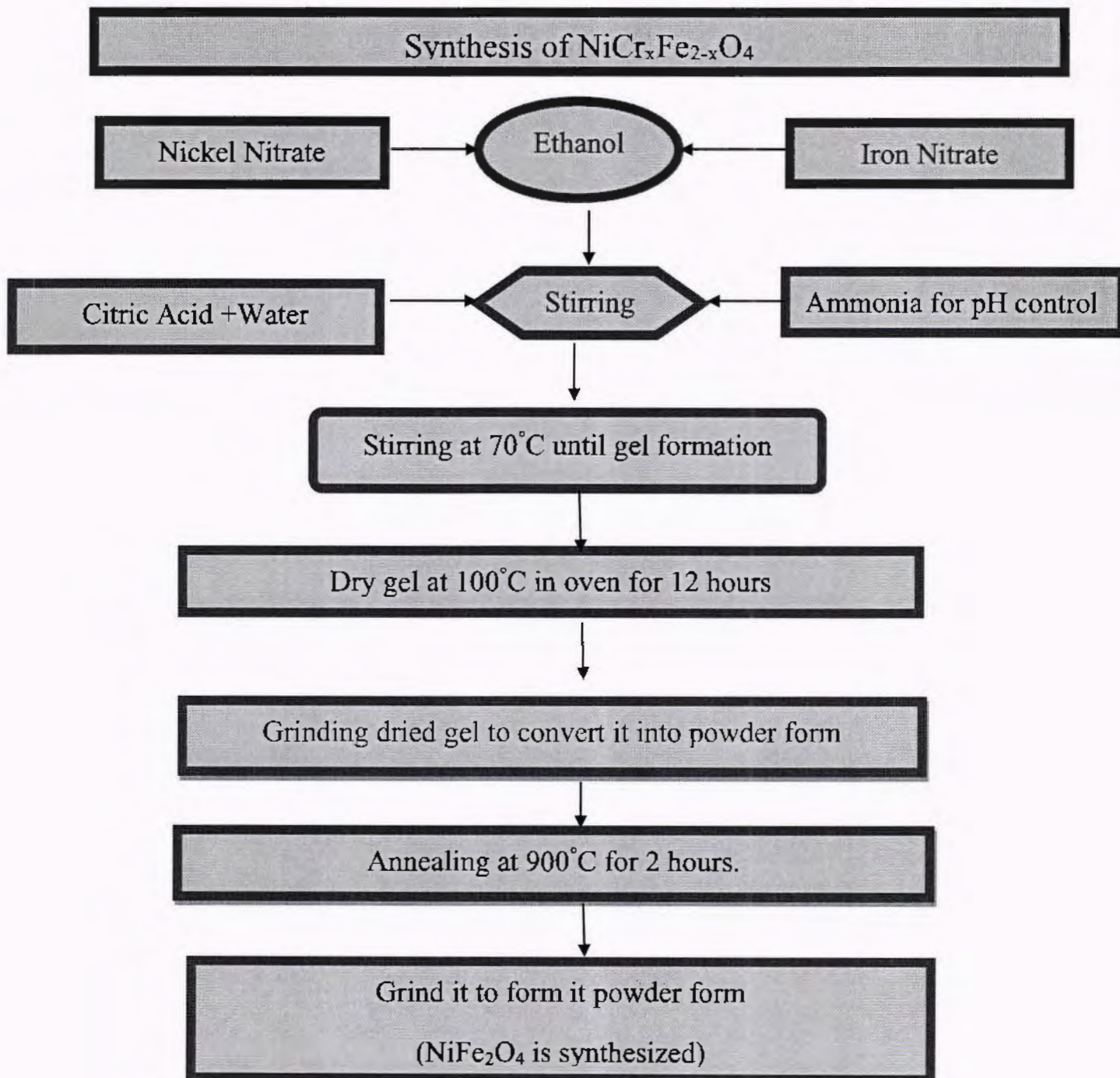
It is bottom up approach. Nickel ferrites (NiFe_2O_4) nanoparticles are prepared by sol-gel method. This method was adopted because it is very versatile and easy method.

TH/18387

By this method fine nanoparticles can be obtained and have the homogeneous dispersion. Required temperature for the synthesis is also not very high.

3.2.1 Flow chart and explanation

The flow chart diagram for the preparation of nickel ferrites nanoparticles is given below.



Chemical used in this method for the synthesis of nickel ferrites are given below.

- Nickel Nitrate ($\text{Ni}(\text{NO}_3)_2 \cdot 6\text{H}_2\text{O}$)
- Iron nitrate ($\text{Fe}(\text{NO}_3)_3 \cdot 9\text{H}_2\text{O}$)
- Ethanol ($\text{C}_2\text{H}_6\text{O}$)
- Citric acid ($\text{C}_6\text{H}_8\text{O}_7$)
- Distilled water (H_2O)
- Ammonia (NH_3)

Nickel nitrate and iron nitrate was taken at the ratio 1:2 and mixed in a beaker. Ethanol was added in the beaker in appropriate amount. The beaker was put on the stirrer so that nickel nitrate and iron nitrate mixed properly. Now citric acid and distilled water was taken in fix ratio and mixed in another beaker and put on the stirrer. After that both solutions were mixed together and again put on the stirrer. Now ammonia was introduced drop by drop until the pH of solution became 5. After that the temperature of 70°C was applied until solution was converted in gel type. This gel was put into the oven at 100°C for 12 hours. After that gel was solidify. Now that solid was grinded and powder was obtained. This powder was placed in the furnace at 900°C for 2 hours. After 2 hours furnace was switched off and when furnace get cooled down to room temperature the sample taken from furnace. Now the sample was grinded and was ready for analysis.

Now for further study Cr^{+3} was chosen as a dopant material. This was doped on B site (octahedral site because of its trivalent nature) at the ratios 0.2wt%, 0.4wt%, 0.6wt%, 0.8wt% and 2.0wt% by using the same process as given above.

3.3 Characterization techniques

Many techniques have been used for the analysis of sample. To determine the crystal structure X-ray diffraction is used. SEM is used for the surface study, EDX for the compositional analysis, TEM for internal morphology, dielectric properties also been measured by LCR meter. Detail of these characterization techniques is given below.

3.4 X-Ray Diffraction (XRD)

X-ray diffraction is used for the identification of phase of any material. It can also give the information about the dimensions of unit cell and its parameters, crystallite size, concentration of impurities, degree of crystallinity and structural defects of samples[41].

To study the solids structure X-ray diffraction is the earliest method. In this method electromagnetic waves having different phases interact with the given material or specimen and produce constructive or destructive interference. In constructive interference bright spots are form on the screen and in destructive interference dark spots are appears on the screen. Accurate lattice parameter values can be measure by careful analysis of X-ray diffraction.

3.4.1 X-rays

X-Rays are the electromagnetic radiations which were discovered in 1885 by the German physiest named as Sir W.C Roentgen. They have the name X-rays because at that time their nature was unknown. X-rays have wavelength of about 1\AA that is nearly equal to the size of an atom and have very high energy that is in the range of 100eV to 100keV.

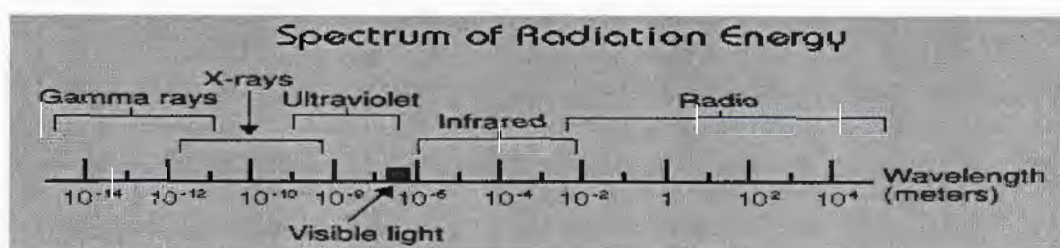


Fig 3.1: Electromagnetic spectrum.

The wavelength of x-rays lies from 0.5\AA to 2.5\AA which is shorter than ultraviolet and their wavelength is larger than gamma rays. This wavelength is same as that of solids materials [42]. By the discovery of X-rays scientist become able to investigate the structure of material at atomic level.

For two main purposes X-Rays diffraction is used, characterization of material as fingerprint and structure determination of the material i.e packing of atoms, angles of atoms and interatomic distance between the atoms. XRD is very key characterization means in material science. By using XRD technique any material's shape and size can be easily determined.

3.4.2 Production of X-Rays

The X-Ray tube is an important source to produce electromagnetic radiation. Electrons are emitted thermodynamically in X-ray tube in which source of copper K_{α} as a target element having wavelength 1.54\AA is used [43]. These emitted electrons are bombarded on the target material or specimen. As a result inner shell transition takes place in a material to produce X-rays. These rays are of different energy. The rays have energy smaller than 10keV are known as soft X-rays while the rays having energy greater than 10keV are named as hard X-rays.

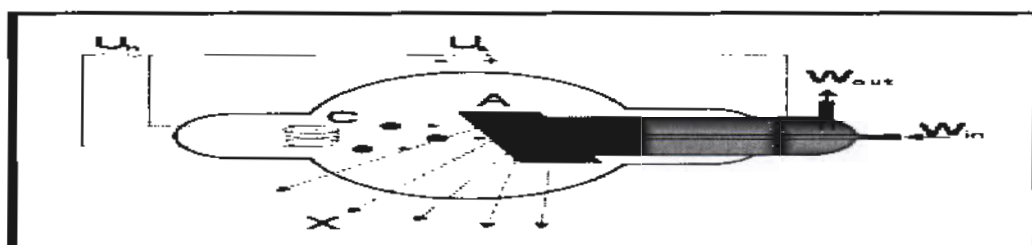


Fig 3.2: Mechanism of X-rays production[43].

For the X-rays production three main sources are required which are given below

- Electrons source
- High voltage source to accelerate the electrons
- Metal target

3.4.3 Bragg's law

W.H Bragg and his son W.L Bragg derived the Bragg's law in 1915. Braggs were given a noble prize on determining the structure of ZnS, NaCl and diamond. This law gives detail about the interference pattern of scattered X-rays by a crystal. Bragg's law states that diffraction will occurs only when following given equation will fulfilled.

$$n\lambda = 2d\sin\theta \quad (3.1)$$

Here "n" is the positive integer, θ is the angle between plane and incident rays (here incident ray and reflected ray obeys the law of reflection), λ is the wavelength of applied x-rays and d is the separation between the planes of specimen[44].

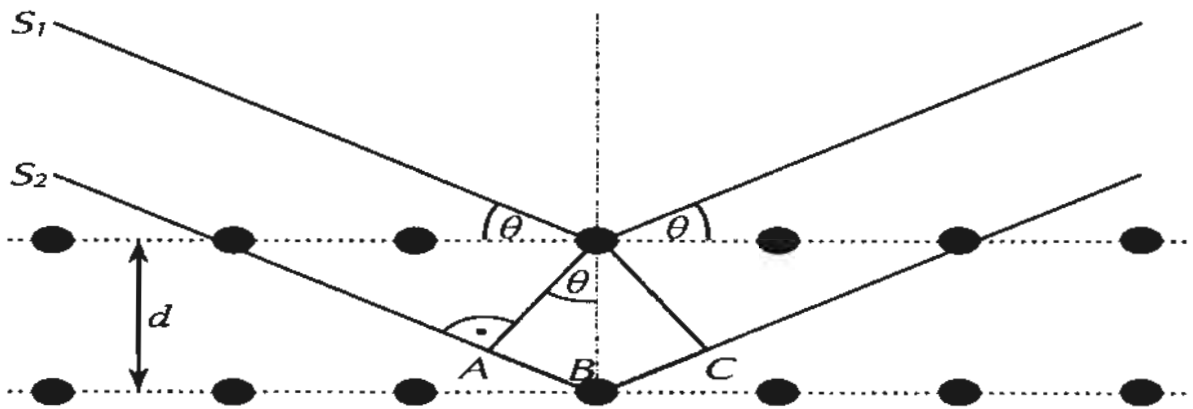


Fig. 3.3: Diffraction of Rays from the plans of crystal[44].

Here the ray S₂ covers the distance larger than ray S₁. This traveled distance depends on the angle of incidence of the rays and distance between the planes of sample/specimen. For interference, path difference of rays must be the integral multiple of wavelength.

Bragg's law can also be written as

$$\lambda = 2d'\sin\theta \quad (3.2)$$

This equation is not include "n" because here $d' = d/n$.

3.4.4 Measurement of particle size

For the measurement of the size of the particle we can use the well known formula known as Debye Scherrer formula. In 1918 Paul Scherrer introduced this

formula. The result of Scherrer formula is comparatively better than the transmission electron microscope. By Scherrer formula we can measure the grain size of 0.1-0.2 μm .

Scherrer formula is given as.

$$D = \frac{0.9\lambda}{B \cos \theta_B} \quad (3.3)$$

Where,

D is the particle size

λ is the wavelength of copper $K\alpha$.

B corresponds to half of the maximum wavelength as given in following figure.

θ_B is the Bragg's angle

Crystal thickness has inverse relation with width of crystal (B) i.e. as B increase size of the particle will decrease [45]

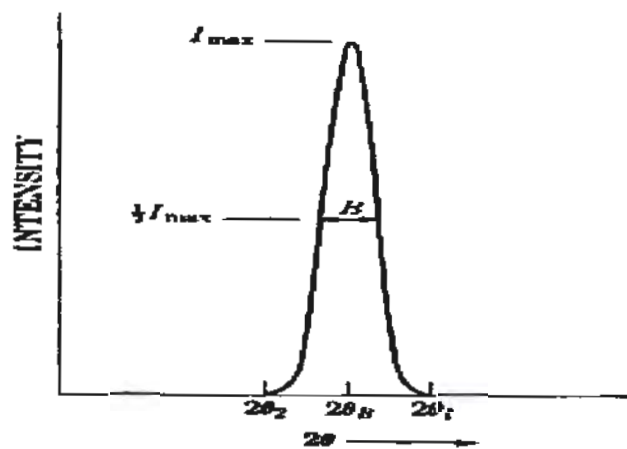


Fig 3.4: FWHM [45].

For the value of B, relation is given below

$$B = \frac{1}{2}(2\theta_1 - 2\theta_2) \quad (3.4)$$

3.5 Fourier Transform Infrared Spectroscopy (FTIR)

“FTIR” is an important technique for identification of material and to study the nature of vibration of its constituents. Infrared radiations are utilized to get already selected objectives. To study the structure of ferrites, infrared radiation having frequency range (350cm⁻¹---700cm⁻¹) are required. When these radiations introduced to the sample some part of these absorbed by the material and some of that transmit. By combining transmitted and absorbed radiation a spectrum is obtained. The spectrum contains information about nature and properties of sample. As every material has their own band orientation so each material have unique spectrum. Michelson Interferometer is a key part of infrared spectroscopy[46].

Following figure (3.5) shows the FTIR apparatus

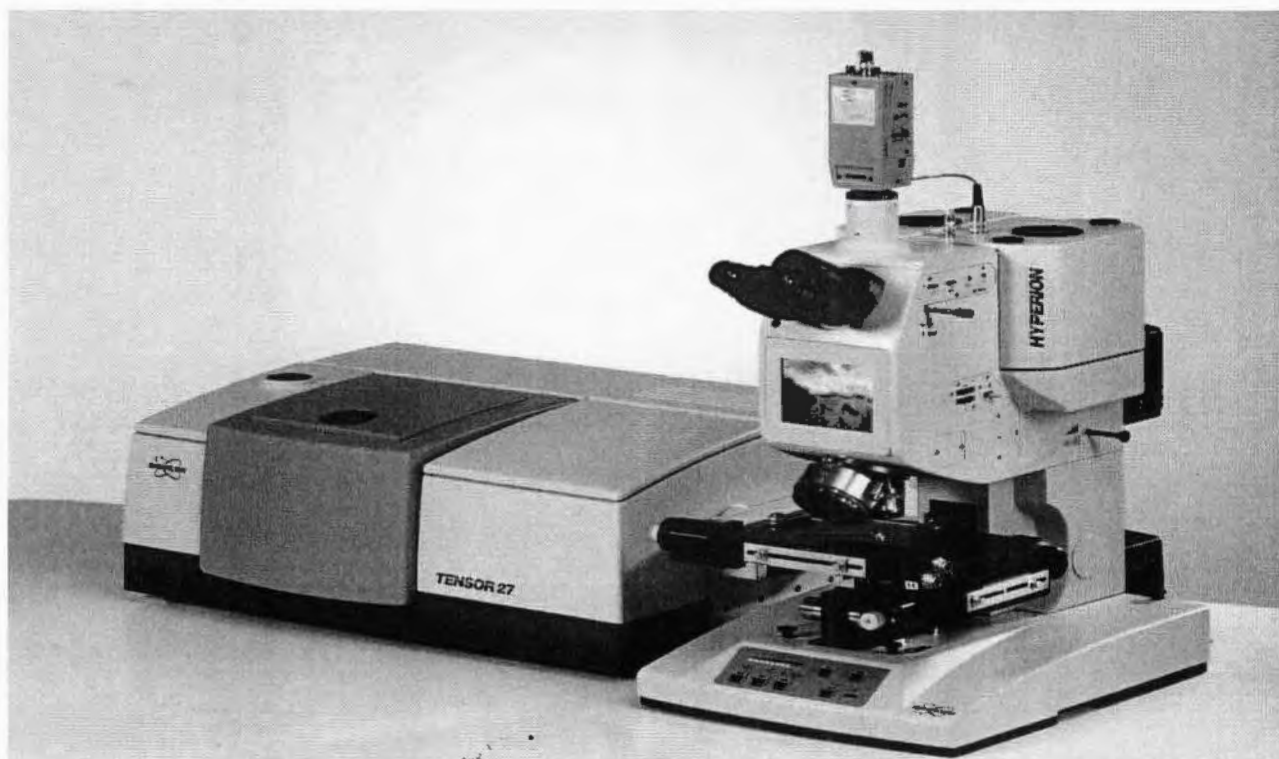


Fig. 3.5: Fourier transform infrared spectroscopy (FTIR) [46].

3.5.1 Michelson interferomete

Michelson interferometer consists of two mirrors in which one is fixed mirror (M1) and one is moveable mirror (M2), a beam splitter and a screen. Experimental setup

of Michelson is shown in the figure (3.6). A beam coming from the source splits into two parts, half transmits and half reflects from the beam splitter and both rays move towards the adjusted mirrors. Reflected ray is moving towards the fix mirror M1 and it reflects again with the same distance and transmitted ray moves towards the moving mirror M2 and reflects with changing distance. Now after reflection these two rays again meet and form interference pattern and this pattern will be detected on the screen for the material analysis [46].

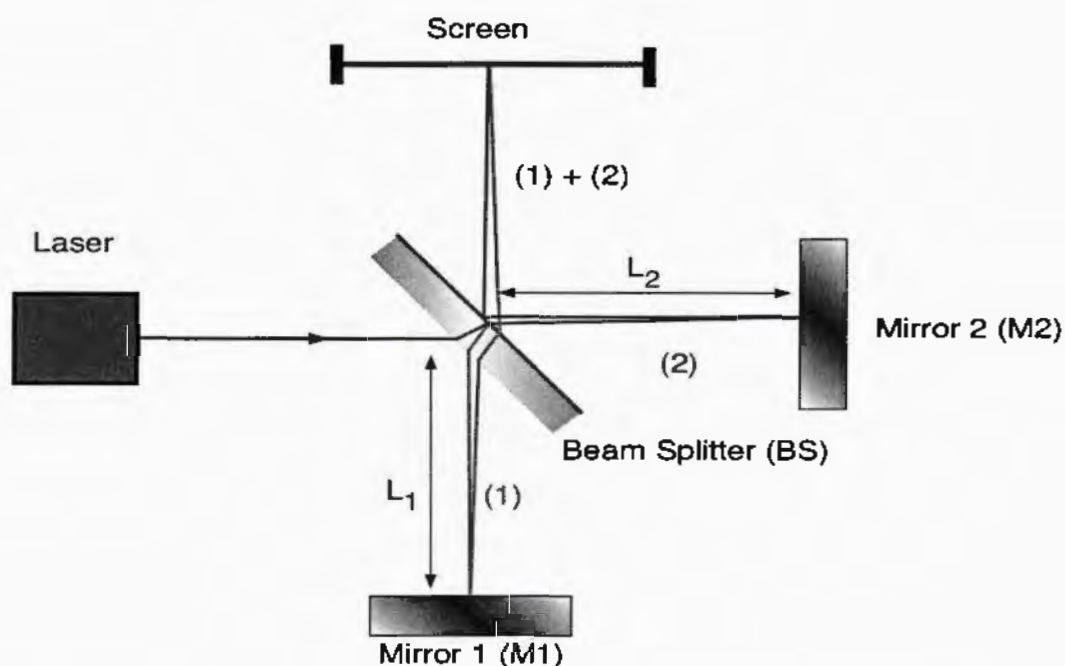


Fig.3.6: Experimental arrangement of Michelson interferometer[46].

3.5.2 Beam splitter

This is semi opaque and semi transparent glass for the infrared radiations. Reflected ray is moving towards the fix mirror and it reflects again with the same distance and transmitted ray moves towards the moving mirror and reflects with changing distance. Now after reflection these two rays again meet and form interference pattern.

3.6 Transmission Electron Microscopy

Transmission electron microscopy is an incredible mean to observe hidden part of microscopic world. TEM is used to observe the internal morphology of sample. It

exposed the amazing progress in the field of science. In TEM we use beam of electron for the imaging of sample. Three dimensional magnified image of a sample can be obtained by TEM that cannot be obtained by optical microscope.

Ernst Ruska and Max Knoll built the TEM in 1931 and in 1939 the first TEM was commercialized [47]. For the development of TEM Ernst Ruska was awarded by the Nobel Prize.

3.6.1 Component of TEM

There are different components of TEM which are given below:

3.6.1.1 Electron gun

Electron gun is the source that produces electrons. These electrons are generated through the tungsten filament at 2700K. These electrons are called thermoelectrons. This filament acts as a cathode. There is Wehnelt outside the filament that gathered the electrons in straight line.

3.6.1.2 Condenser lens and condenser aperture

The magnetic lenses are placed below the electron gun. The purpose of lens is to adjust the width of the electrons beam. A narrow beam of electron is necessary for the transmission electron microscopy. When we have greater the strength of lens then diameter of electron beam will be small and vice versa.

Condenser aperture is used to control the number of electrons reaching to the sample. It excludes the high angled electrons.

3.6.1.3 Objective lens

After passing through the specimen the electron beam will scattered due to the electrostatic potential of the constituent elements of the sample/specimen, then here objective lens is used to focus this electron beam and determines the final diameter of the electron beam. It focuses the electron beam on the CCD or phosphor screen. Objective aperture can also be used to control the high angled electrons.

3.6.1.3 Intermediate lens

The purpose of intermediate lens is to magnify the early image that is formed by the objective lens.

3.6.4.4 Projector lens

Projector lens further magnifies the image after magnification from the intermediate lens.

3.6.4.5 Image observation

Now image can be observe on the screen in the chamber or by camera mounted below the column[47].

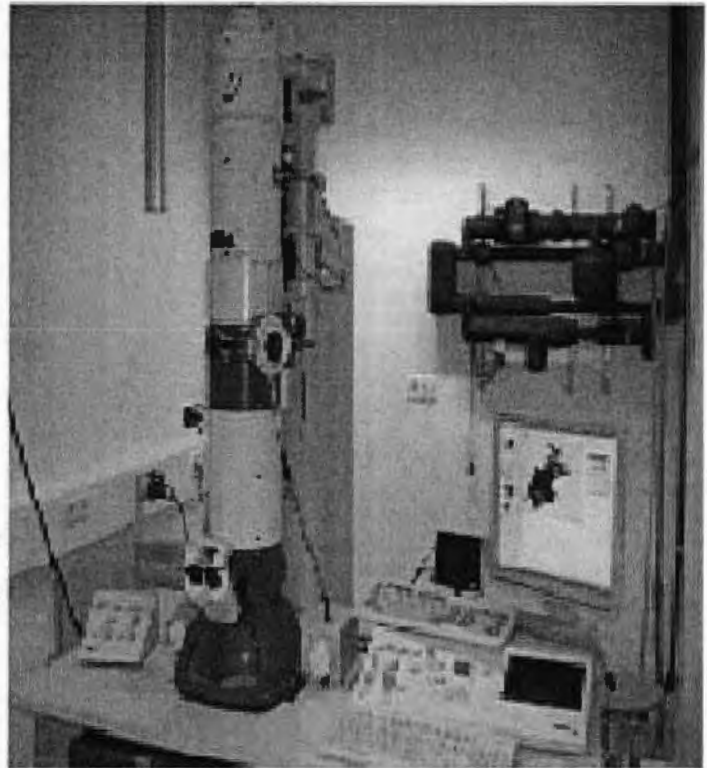
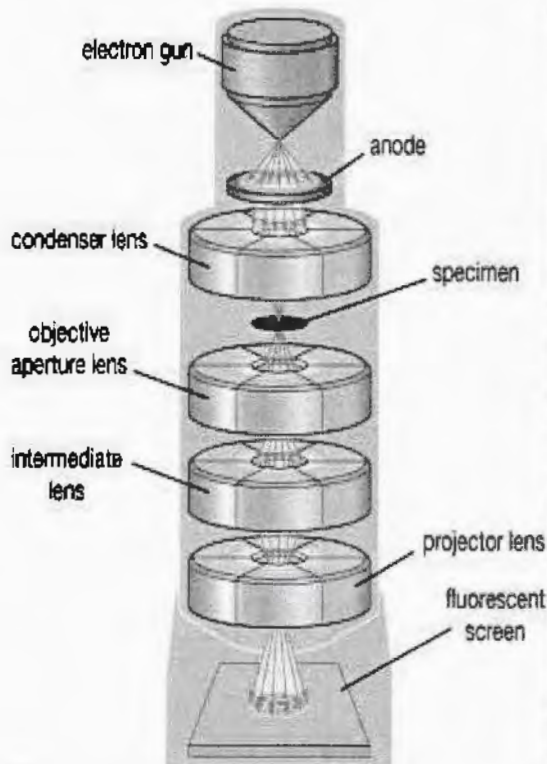


Fig 3.7: (a) Working principle of TEM (b) Transmission Electron Microscope[48].

3.6.2 Working principle of TEM

The electrons are emitted from the filament (mostly tungsten filament) by heating the filament. Now emitted electrons, in the form of beam flow down the column towards the sample/specimen. But this beam is scattered, to focus this beam it passes the condenser lens. After passing of electron beam from the lens, it becomes sharp and focused. These focused electrons fall on the specimen and a part of beam gets transmitted from the sample. This transmitted beam is again focused by the objective lens and fall on the screen. After this intermediate lens and projector lens magnify the image. The figure 3.5(a) shows the working of TEM and figure 3.5(b) is the TEM machine.

3.7 Energy Dispersive X-rays Spectroscopy (EDX or EDS)

EDX is a procedure that is used for the elemental composition, investigation and chemical characterization any sample. In EDX a beam of energetic electrons fall on the sample. When the high energy beam of electrons strike the target sample then the ground state electron (unexcited electrons) from the inner energy level may get knocked out and creates vacancy. To fill this vacancy an electron from the higher energy level will jump into the lower energy level by emitting the extra energy that is equal to the difference of these two energy levels in the form of X-rays. These X-rays are detected by the energy dispersive spectrometer/detector. This detector converts the incoming x rays into electrical pulse. After that these pulses of different amplitude are count by the signal processing electronic resulting in the histogram of x rays energy versus intensity. Now as every atom has X-rays of different wavelength so by comparing we can find the elemental composition of the sample[49].

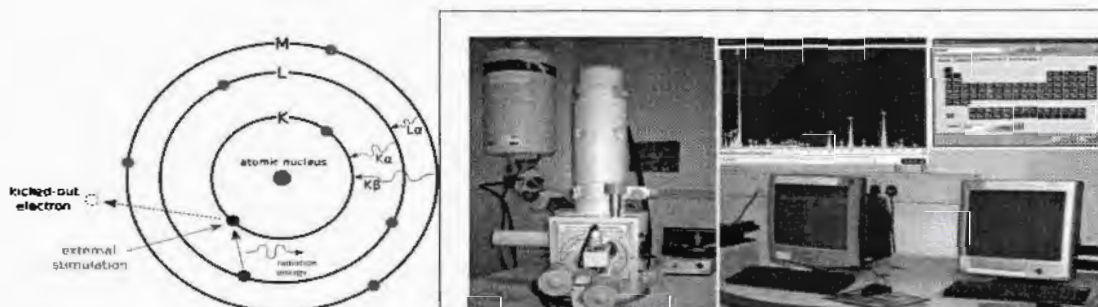


Fig 3.8: (a) Energy dispersive (b) X-rays Spectroscopy[49].

3.8 LCR Meter

LCR stands for inductance (L), resistance(R) and capacitance(C). LRC meter is a device which is used to measure the dielectric properties of the sample. It also measure capacitance, inductance and resistance of a sample. The following figure shows the Wayne Kerr 6440B LCR meter from NUST used for dielectric measurement. The frequency range of this meter is 100Hz to 5MHz. it gives the dissipation factor and capacitance for each value of frequency. The capacitance and dissipation factor can be measure by single frequency mode LCR meter while resistance, inductance and capacitance can be measured by multi frequency mode LCR meter.[50]

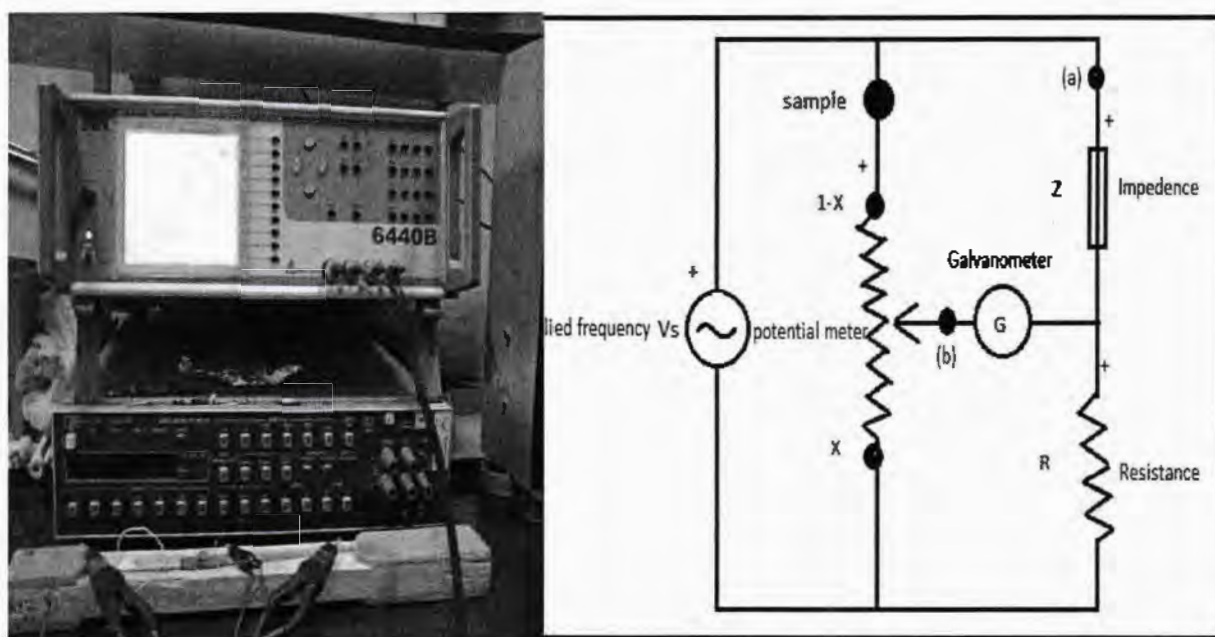


Fig 3.9: (a) LRC meter 6440B (b) Circuit diagram of bridge of LCR meter .

There are two types of LCR meter which are handheld and benchtop LCR meter.

3.8.1 Handheld LCR meter

Handheld LCR meter is a convenient, lightweight, smart LCR meter. It operates on small voltage. Advance handheld LCR meter has advance features e.g it can support the USB to log data to computer. By using handheld LCR meter we can quickly perform the LCR measurements accurately

3.8.2 Benchtop LCR meter

Benchtop LCR meters are prominent because of their accurate analysis upto 0.01% and controllable frequency. They are directly control by the computer. More important thing of benchtop LCR meter is DC bias current/voltage.

Results and discussion

Ferrite nanoparticles gain an incredible attraction in the recent research because they are very valuable in technological applications. They consist of normal, mixed and inverse spinel structures. At nano level, ferrite nanoparticles show amazing and outstanding properties which are not observed in the material at bulk level because of high surface to volume ratio [51]. Among such nanoparticles, Nickel ferrite nanoparticles are unique due to practical applications in different fields such as data storage, drug deliveries and transformers cores.

Doping in ferrite nanoparticles have very interesting role in controlling the physical properties of ferrite nanoparticles. The doping at B site may cause the cationic distribution between A and B site which can alter the physical properties of ferrite nanoparticles. The doping of antiferromagnetic Cr^{+3} at B site of NiFe_2O_4 nanoparticles can control structure stability which can enhance dielectric properties of NiFe_2O_4 nanoparticles. So, it is very interesting to study the synthesis and characterization of NiFe_2O_4 nanoparticles. We have synthesized nanoparticles by Sol gel method and study the effect of Cr^{+3} doping on dielectric properties of NiFe_2O_4 nanoparticles. Different characterization techniques such as X-ray diffraction (XRD), Furrier transform infrared (FTIR), Energy dispersive x-ray spectroscopy (EDX), Transmission electron microscopy (TEM) and LCR meter are used for the analysis of the nanoparticles.

4.1 X-Ray diffraction (XRD)

X- ray diffraction (XRD) is a non-destructive characterization tool which gives information about crystal structure, crystallite size and lattice parameter of nanoparticles. Fig. 4.1 shows XRD pattern of $\text{NiCr}_x\text{Fe}_{2-x}\text{O}_4$ nanoparticles where $x=0, 0.2, 0.4, 0.6, 0.8$ and 2. The diffracted peaks (1 1 1), (2 2 0), (3 1 1), (2 2 2), (4 0 0), (4 2 2), (5 1 1), (4 4 0) and (5 3 3) are the miller indices of pure $\text{NiCr}_x\text{Fe}_{2-x}\text{O}_4$ nanoparticles at different angles, $2\theta = 18.5^\circ, 30.4^\circ, 35.7^\circ, 37.4^\circ, 43.4^\circ, 54^\circ, 57.5^\circ, 63.1^\circ$ and 74.6° respectively for all samples. $\text{NiCr}_x\text{Fe}_{2-x}\text{O}_4$ XRD pattern shows cubic spinel structure for all samples [52]. All the

major peaks of NiFe_2O_4 remain unchanged after the Cr dopant. There were no impurity phases detected in all samples which confirm the single phase $\text{NiCr}_x\text{Fe}_{2-x}\text{O}_4$ nanoparticles.

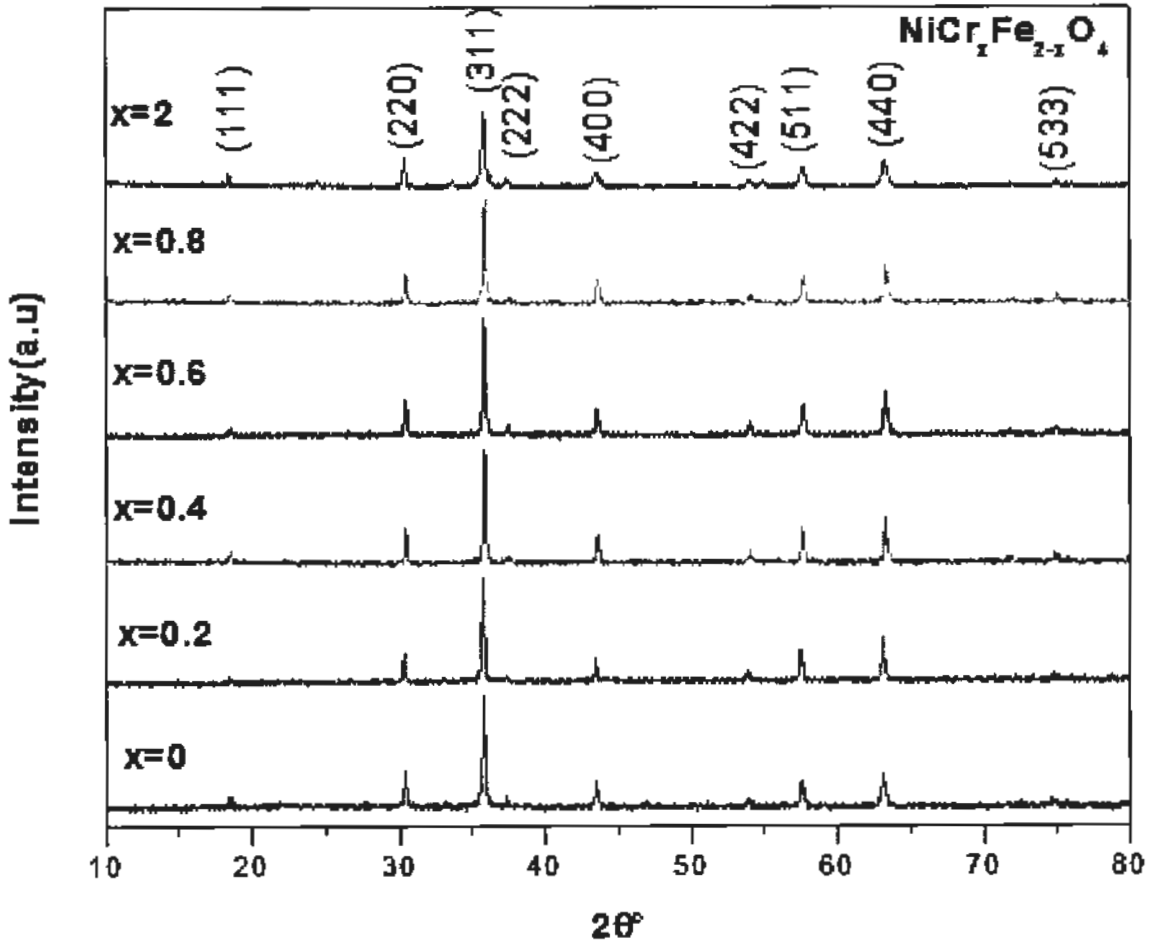


Fig. 4.1: XRD pattern of $\text{NiCr}_x\text{Fe}_{2-x}\text{O}_4$ for $x=0, 0.2, 0.4, 0.6, 0.8$ and 2 .

The crystallite size of nanoparticles of $\text{NiCr}_x\text{Fe}_{2-x}\text{O}_4$ was measured by the help of Debye Scherrer's formula given below[52].

$$D = 0.9\lambda/\beta \cos \theta \quad (4.1)$$

Here β is the full width at half maximum (FWHM) of the peak of XRD, θ is the Bragg angle and λ is the wavelength of X-rays. Fig. 4.2 (a) shows the calculated crystallite size of $\text{NiCr}_x\text{Fe}_{2-x}\text{O}_4$ nanoparticles at $x=0, 0.2, 0.4, 0.6, 0.8$ and 2 . The crystallite size was found to be in the range of 28 nm to 44 nm. The maximum crystallite size was observed for $x=0$ concentration and then decreased for all the concentration of Cr.

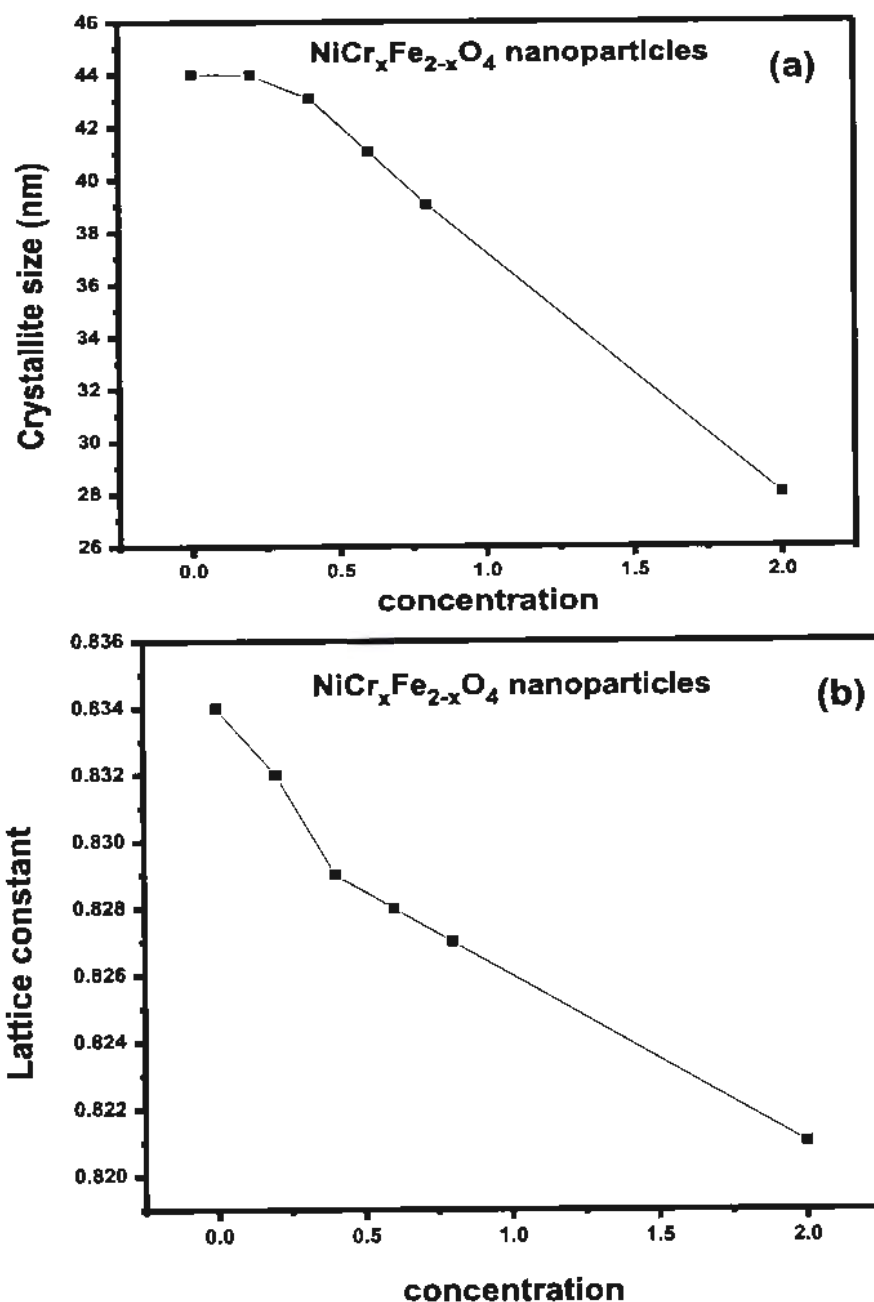


Fig 4.2(a): Crystallite size of $\text{NiCr}_x\text{Fe}_{2-x}\text{O}_4$ (b) Lattice constant of $\text{NiCr}_x\text{Fe}_{2-x}\text{O}_4$.

Lattice constant was calculated by the help of following formula[53].

$$a = d(h^2+k^2+l^2)^{1/2} \quad (4.2)$$

Where (h k l) are the miller indices and “d” is interplanar space which can be calculated by the help of Bragg’s law. Bragg’s law is given as

$$n \lambda = 2d \sin \theta$$

For n=1

$$\lambda = 2d \sin \theta \quad (4.3)$$

Fig. 4.2 (h) shows value of lattice parameter for $\text{NiCr}_x\text{Fe}_{2-x}\text{O}_4$ nanoparticles. It has been observed that the value of lattice parameter has decreased very slightly with the doping of Cr. It is due the replacement of larger ionic radius crystal Fe^{2+} (0.67 Å) by the smaller Cr^{3+} (0.64 Å)[54]. Due to the strong preference of Cr^{3+} ions for octahedral site, it must have replaced the Fe^{3+} ions at octahedral and has not disturbed the spinal cubic structure of $\text{NiCr}_x\text{Fe}_{2-x}\text{O}_4$ nanoparticles.

4.2 Fourier transform infrared (FTIR) analysis

Fourier transform infrared (FTIR) spectroscopy is used to study the nature of chemical bond in nanoparticles. Fig. 4.3 shows the room temperature FTIR spectra for $\text{NiCr}_x\text{Fe}_{2-x}\text{O}_4$ nanoparticles in the frequency range 350-750 cm^{-1} . The FT-IR spectra of $\text{NiCr}_x\text{Fe}_{2-x}\text{O}_4$ nanoparticles show two strong absorption bands (ν_1) in the range of 595–622 cm^{-1} and (ν_2) in the range of 400–500 cm^{-1} . The absorption band ν_1 at higher frequency is due to the metal-oxygen vibrations at tetrahedral site (A-site) while the stretching band ν_2 at lower frequency is due to metal-oxygen vibrations at octahedral site (B-site)[55]. The vibrational frequencies of the IR bands corresponding to tetrahedral and octahedral sites are given in Fig 4.3 for different concentration of Cr. It is observed that bands ν_1 and ν_2 shift towards higher wave number with increasing Cr^{3+} ions as compared to Fe^{3+} ions. This shift is due to the reduction in the size of unit cell.

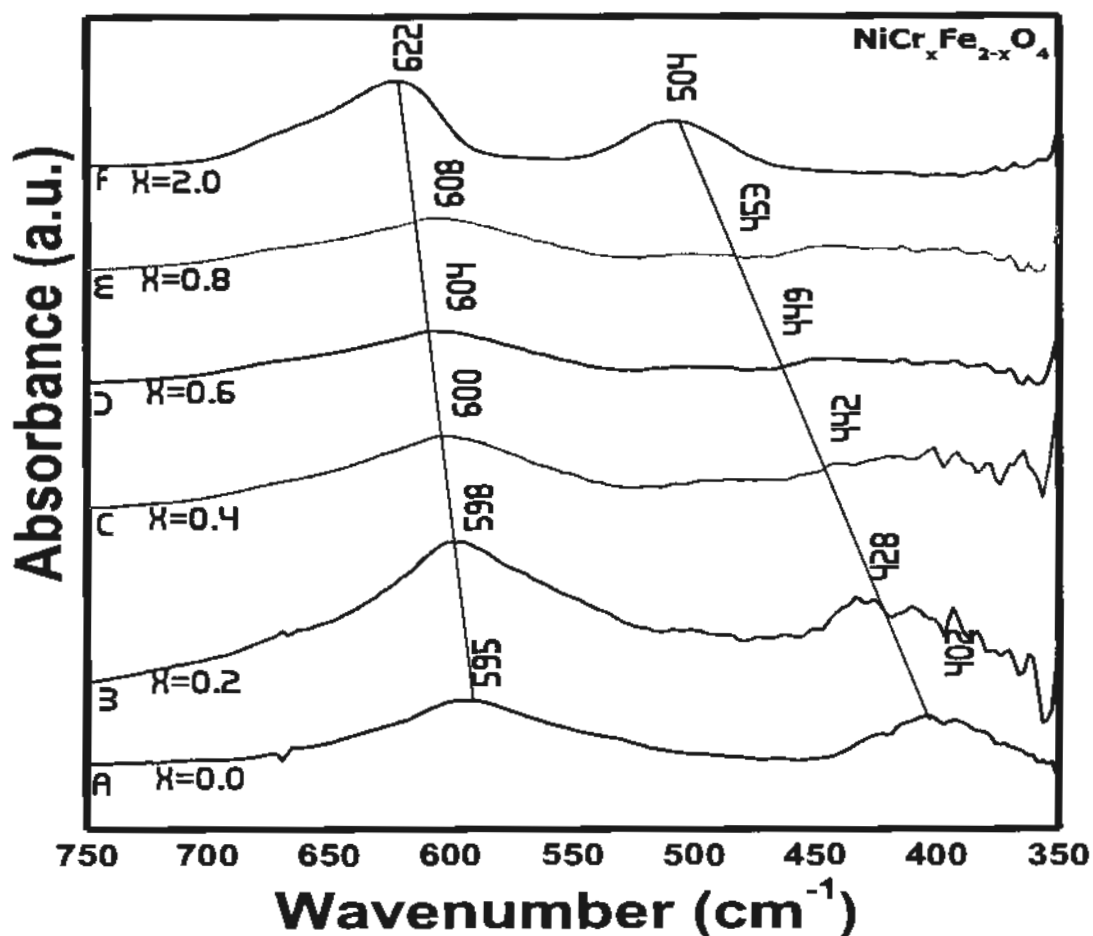


Fig. 4.3: FTIR spectra of $\text{NiCr}_x\text{Fe}_{2-x}\text{O}_4$.

4.3 Energy dispersive spectroscopy (EDX)

Fig. 4.4(a) shows the EDX pattern of NiFe_2O_4 nanoparticles. the peaks of Ni, Fe, O and Al substrate were observed on the EDX image and confirmed the homogeneous mixing of the Ni, Fe, and O atoms in pure ferrites [56]. EDX confirmed the formation of NiFe_2O_4 nanoparticles. The inset table of Fig. 4.4(a) shows the percentage composition of the individual elements in NiFe_2O_4 nanoparticles. Fig. 4.4(b) shows the EDX mapping of the elements Ni, Fe and O. It is found that the observed mass % of metals agree quite well with theoretical metal concentration. Cr and Fe molar concentration of 1:2 was also confirmed by the observed composition.

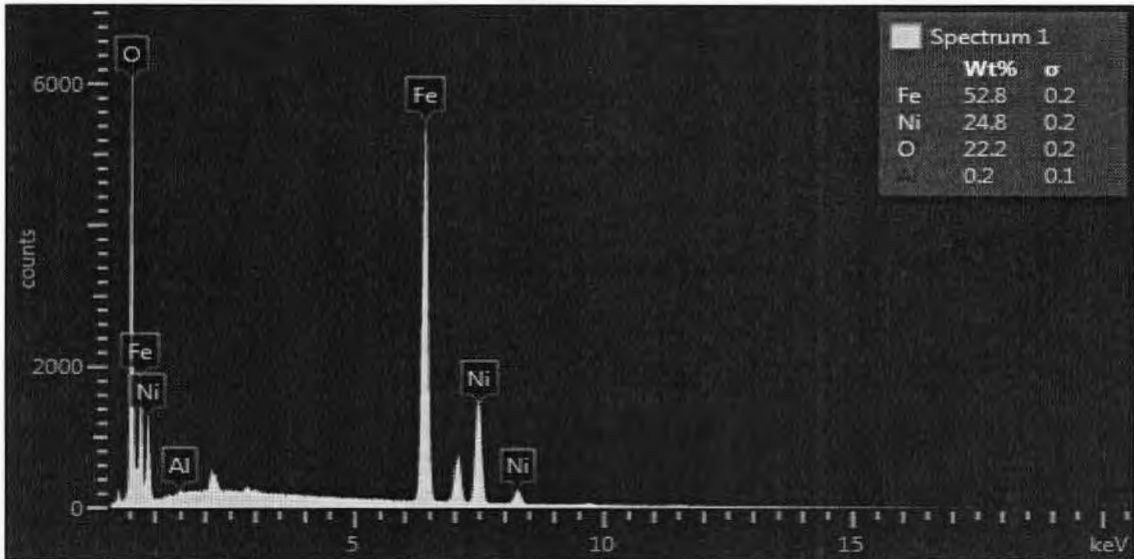
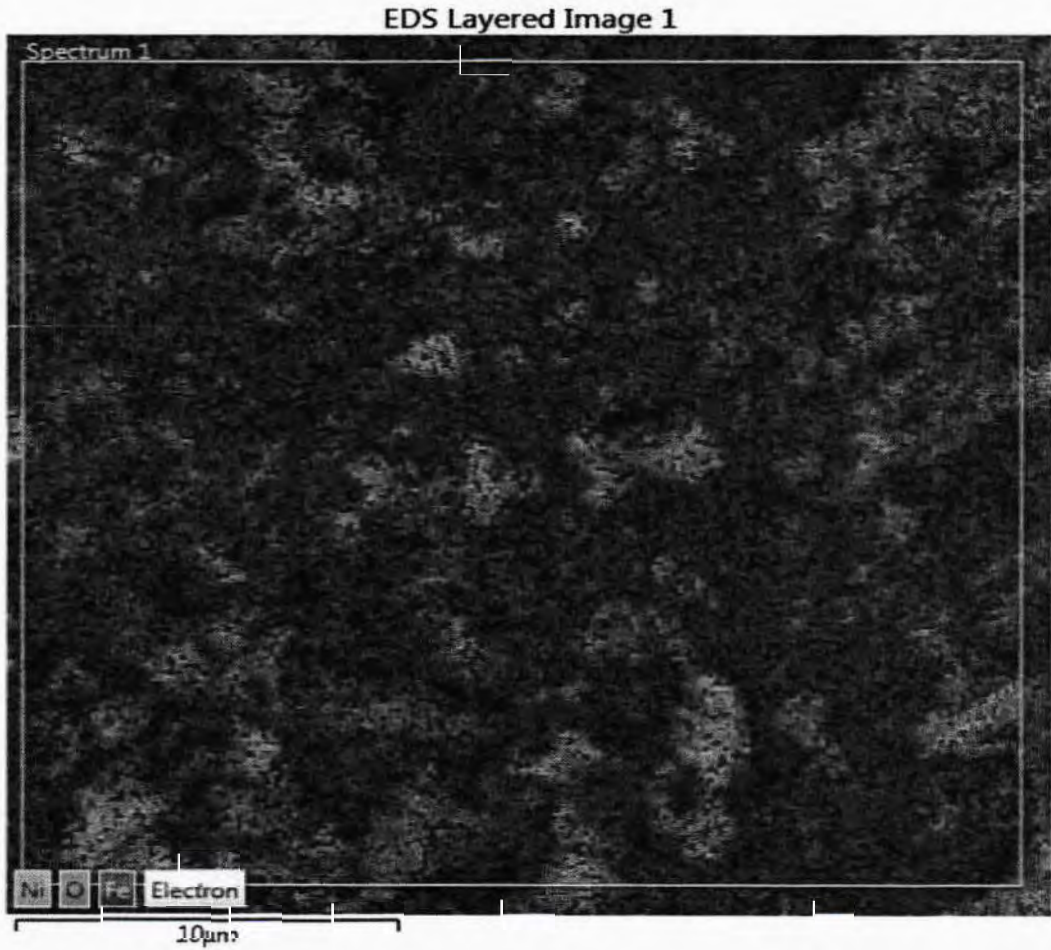


Fig. 4.4(a):EDX of NiFe₂O₄ nanoparticles.



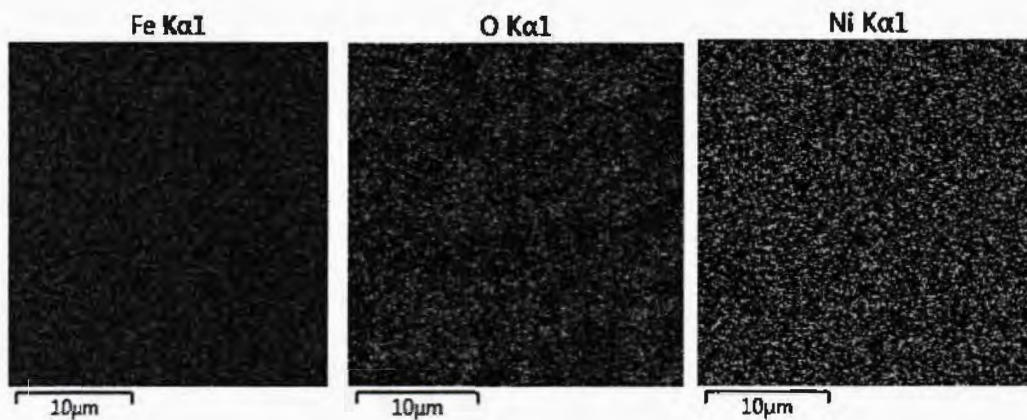


Fig. 4.4(b): Mapping images of NiFe_2O_4 nanoparticles.

4.4 Transmission Electron Microscopy (TEM)

Transmission Electron Microscopy (TEM) scans are used for morphology and average particle size of nanoparticles. Fig. 4.5 shows TEM image NiCr_2O_4 nanoparticles at 100 nm scale. As can be seen from the image that nanoparticles are hexagonal like shape but most of them are irregular shape. The average particle size obtained from TEM image is 47 nm that corresponds well the calculated size of 44 nm from XRD data. The nanoparticles are well dispersed and show less agglomeration[19].

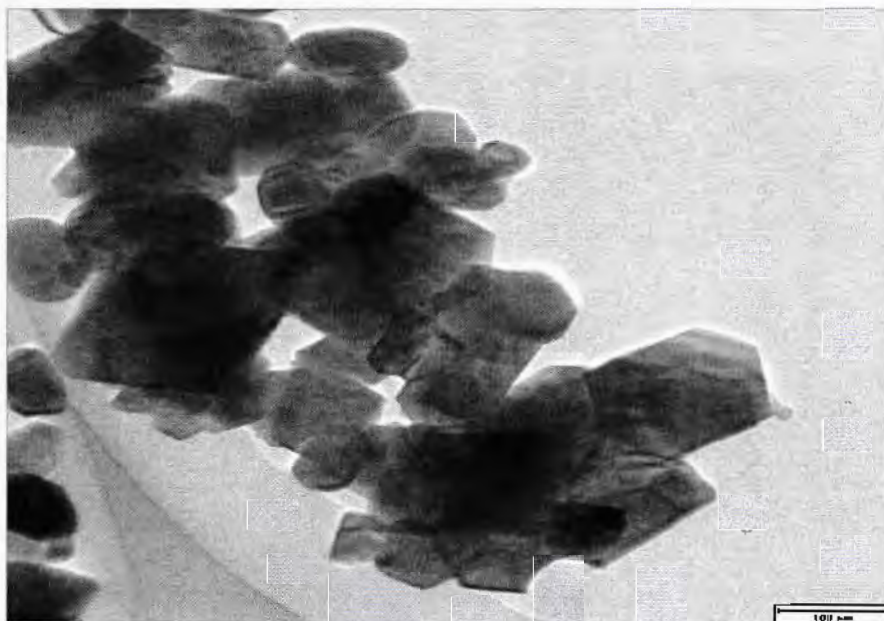


Fig. 4.5: TEM image of $\text{NiCr}_x\text{Fe}_{2-x}\text{O}_4$ ($x=2$) nanoparticles at 100 nm scale.

4.5 Dielectric properties

Dielectric properties of nanoparticles depend on different factors which include process of preparation, chemical composition, annealing temperature, sizes of prepared particles, ratio of dopant particles etc. We have studied the effect of Cr^{+3} doping at octahedral B-site on the dielectric properties of NiFe_2O_4 nanoparticles. The dielectric response was measured with the help of LCR meter in the frequency range of 100 Hz to 5 MHz. Dielectric parameters such as real and imaginary part, dissipation factor or tangent loss and ac conductivity as a function of frequency were measured.

4.5.1 Real part of Dielectric

Fig. 4.6 (a) and (b) show the real part of dielectric constant of pure NiFe_2O_4 and Cr doped NiFe_2O_4 nanoparticles respectively. Real part of dielectric constant of $\text{NiCr}_x\text{Fe}_{2-x}\text{O}_4$ ($x=0, 0.2, 0.4, 0.6, 0.8$ and 2) was calculated using equation.

$$\epsilon' = (c*d) / (\epsilon_0 * A) \quad (4.4)$$

Real part of un-doped and Cr doped NiFe_2O_4 nanoparticles exhibit same behavior. At low frequency range, real part shows maximum value and gradually decrease to low value as the frequency of the applied field increases. The decreasing trend of real part with increasing frequency is typical for ferrites. This behavior can be explained based on polarization namely electronic, ionic, dipolar and space charge polarization. At lower frequency, these types of polarization contribute very well while at higher frequency some polarization types relaxed out, resulting in decreasing the real part of dielectric constant at higher frequency [57]. Maxwell-Wigner and Koop's model further explains this behavior [58]. According to this model, ferrites consist of grains (highly conducting region) and grain boundaries (poorly conductive). At low frequencies, the grain boundaries are more effective in producing polarization because electrons pile up at resistive grain boundary and enhances polarization. At higher frequencies, the lagging behind of charge carriers of grains cannot contribute in polarization of dielectric constant. As a result, real part of dielectric constants decreases at high frequency [59]. In our frequency range, mostly space charge polarization occur and play role in dielectric constant [60].

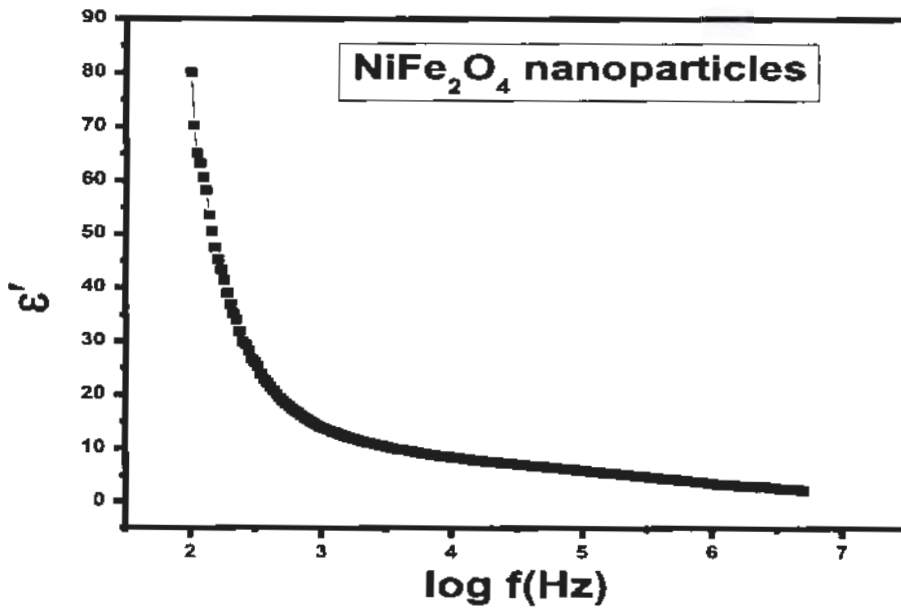


Fig 4.6(a): Real part of dielectric of NiFe₂O₄ nanoparticles.

Fig. 4.6(b) shows the real part of Cr doped nickel ferrite nanoparticles. It can be clearly seen that the value of real part of dielectric increased by doping of Cr⁺³ concentration. This increase is due to fact that chromium is less conductive nature as compare to iron. Conductivity of chromium is $6.7 \cdot 10^6$ S/m and the conductivity of iron is $1 \cdot 10^7$ S/m.

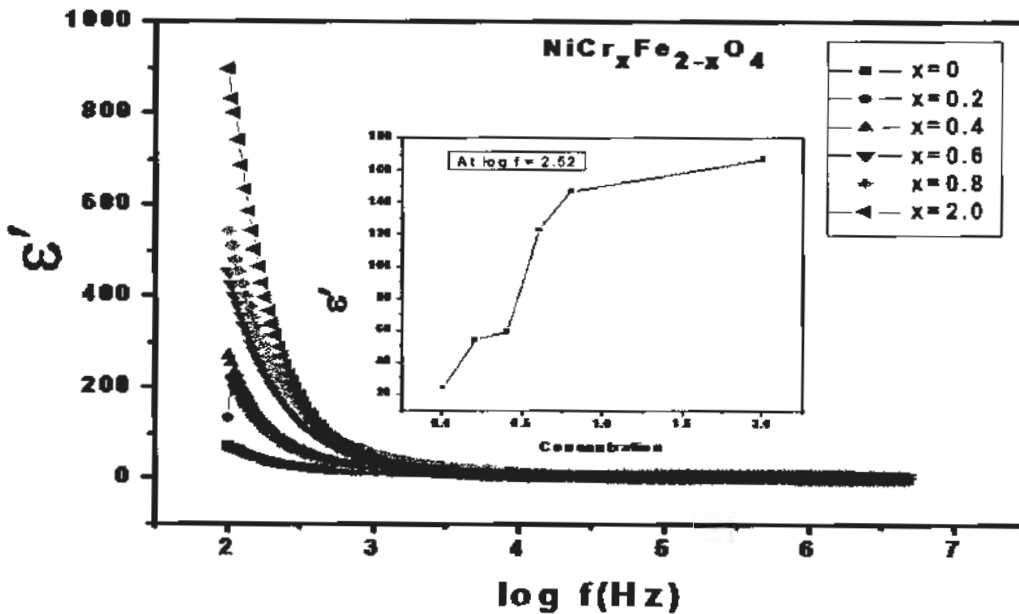


Fig. 4.6(b): Real part of dielectric of NiCr_xFe_{2-x}O₄ nanoparticles.

4.5.2 Imaginary part of Dielectric constant

Imaginary part of dielectric constant can be defined in terms of tangent loss and real part of dielectric constant. Imaginary part was calculated by using the following relation.

$$\epsilon'' = \epsilon' \tan \delta \quad (4.5)$$

Fig. 4.7(a) shows the imaginary part of dielectric of NiFe_2O_4 nanoparticles. In equation, imaginary part depends on tangent loss and real part of dielectric constant. At low frequency the value of imaginary part is high and by raising the frequency up its value is decreased and at high value of frequency the imaginary part becomes almost independent[61]. The imaginary part of dielectric constant also explained based on Maxwell-Wigner and Koop's model. According to Koop's model resistivity is high due to grain boundaries at lower frequencies therefore the energy required for electron hopping between Fe^{2+} and Fe^{3+} ions at the grain boundaries is higher hence the imaginary part is high. On the other hand, at higher frequencies the resistivity is small due to conducting grains that offer negligible resistance to the electron hopping thus energy losses are minute.

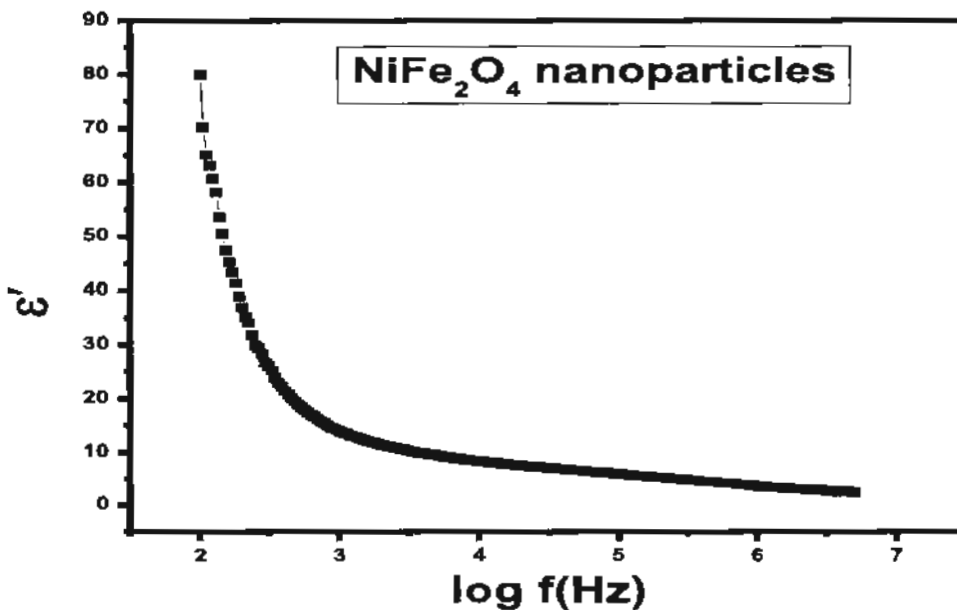


Fig. 4.7(a): Imaginary part of dielectric of NiFe_2O_4 .

Fig. 4.7(b) shows the imaginary part of Cr doped nickel ferrite by doping with Cr^{+3} on octahedral B-site the imaginary part increased. The imaginary part show maximum value for $x=2$ concentration. This is due to less conductive nature of chromium as compare to iron.

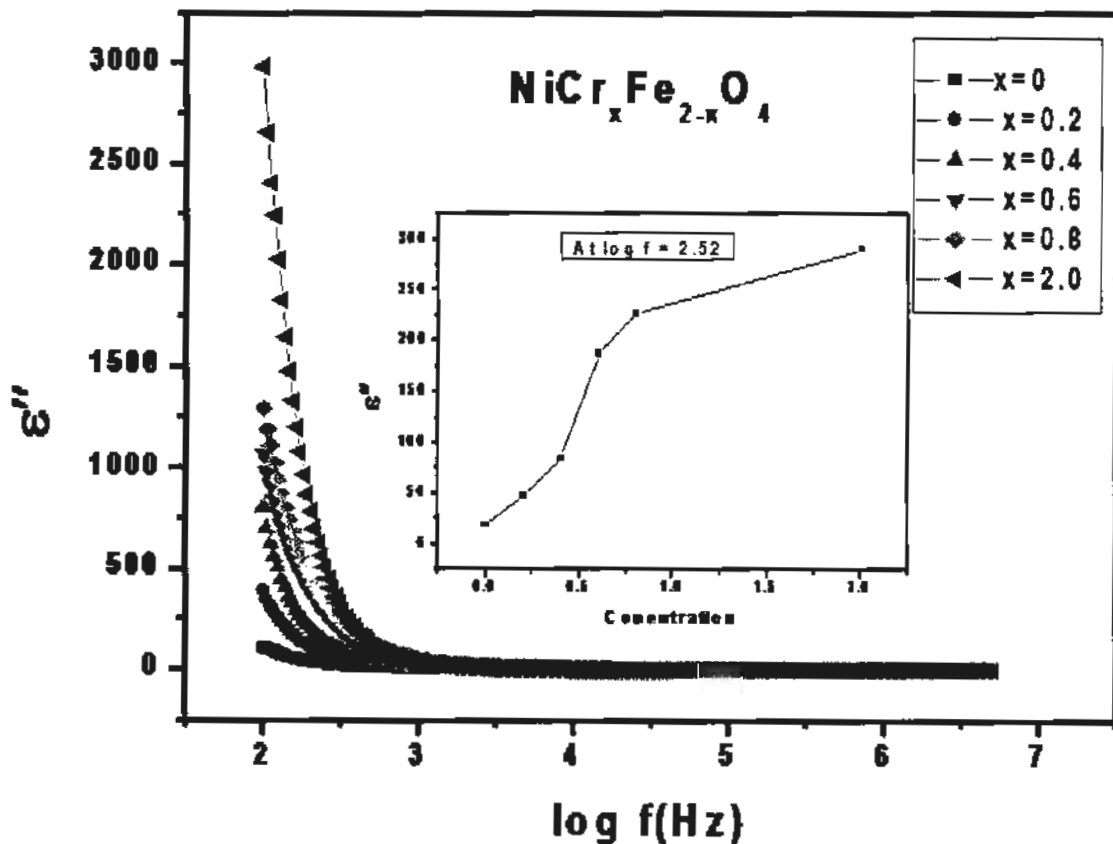


Fig. 4.7(b): Imaginary part of dielectric of $\text{NiCr}_x\text{Fe}_{2-x}\text{O}_4$ nanoparticles.

4.5.3 Dielectric loss tangent

It is also known as dissipation factor ($\tan\delta$). Figure 4.8(a) shows the dielectric loss tangent for pure NiFe_2O_4 nanoparticles. It can be clearly seen that the dielectric loss tangent is high at low frequency and show decreasing trend with increasing frequency. This decrease in dissipation factor can be explained on the basis of Koop's model[58]. At low frequency grain boundaries are effective (which are resistive) and provide more resistance to the electron flow, therefore energy loss is high.

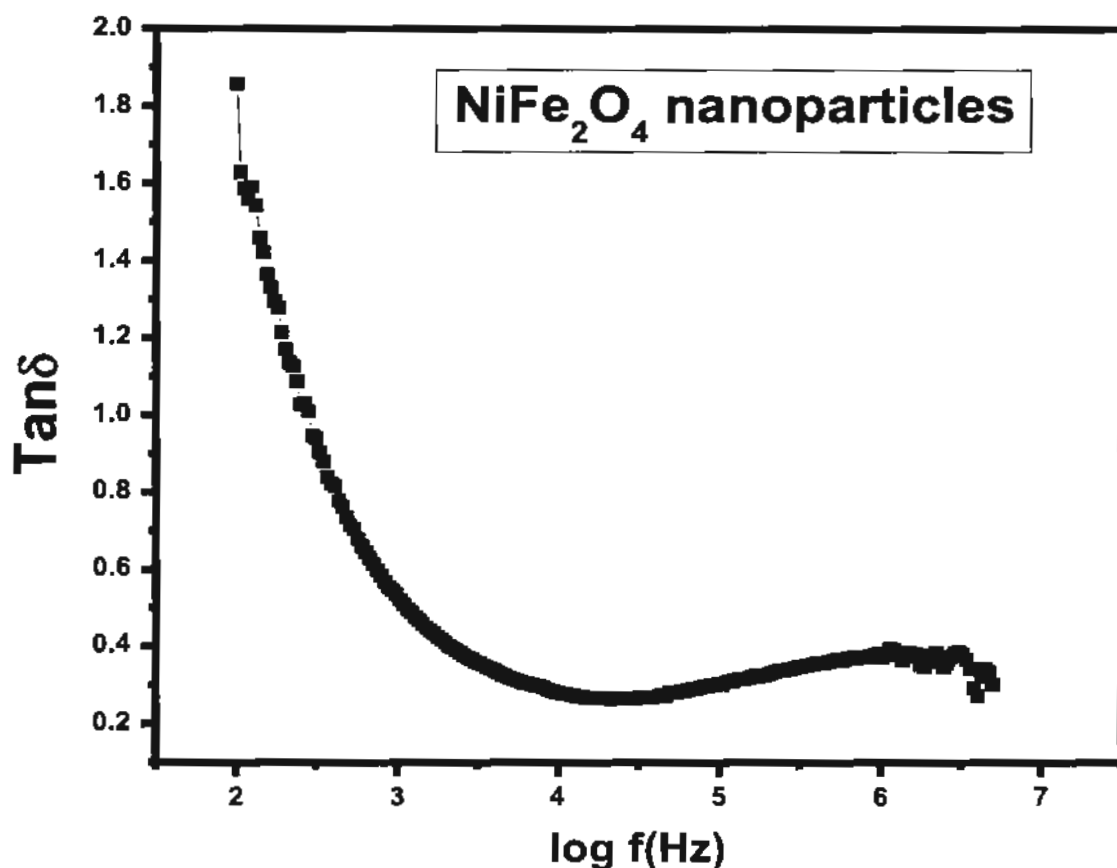


Fig. 4.8(a): Tangent loss of NiFe₂O₄ nanoparticles.

Fig. 4.8(b) shows the dissipation factor of Cr³⁺ doped NiFe₂O₄ nanoparticles. The dissipation factor reveal increasing trend by doping with Cr³⁺ on octahedral site. This is also due to less conductive nature of chromium as compare to iron. From the dielectric measurement, we observed that both dielectric loss factor (imaginary part) and dissipation factor (tangent loss) show similar trend to that of dielectric constant because these dielectric parameters are correlated with each other. Energy dissipation in the dielectric systems is due to dielectric loss angle and dielectric loss factor. These losses originated due to domain wall resonance. Moreover, losses are low at higher frequency since domain wall motion is repressed [62].

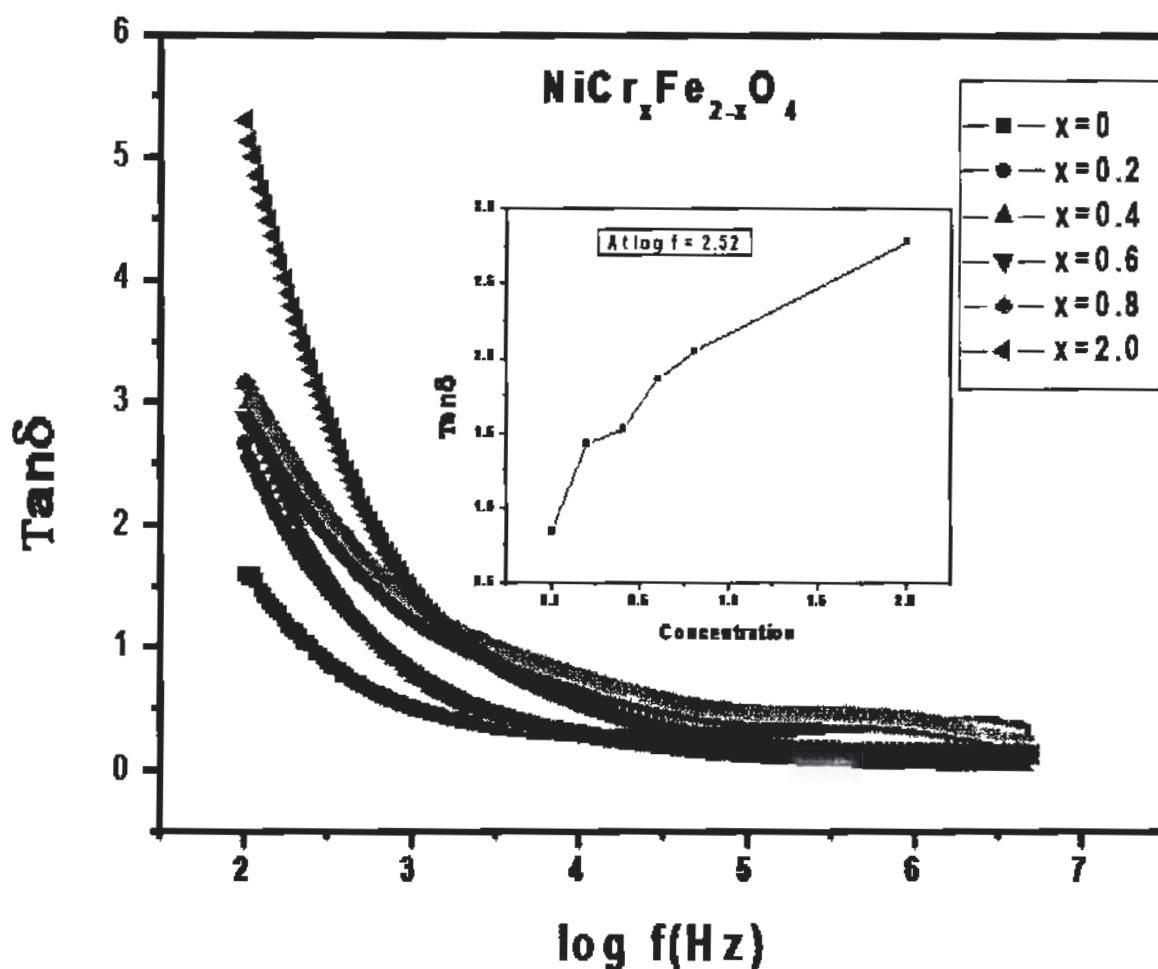


Fig. 4.8(b): Tangent loss of $\text{NiCr}_x\text{Fe}_{2-x}\text{O}_4$ for ($x=0.0, 0.2, 0.4, 0.6, 0.8$ and 2).

4.5.4 AC Conductivity

AC conductivity helps us to understand the conduction mechanism and types of ions responsible for the conduction and it is calculated by the formula given below:

$$\sigma_{ac} = \epsilon' / \epsilon_0 \omega \tan \delta \quad (4.6)$$

Here ϵ' is the real part, ϵ_0 is the free space permittivity, ω is the angular frequency having value $2\pi f$ and the $\tan \delta$ is the dielectric loss tangent.

Fig. 4.9 (a) shows ac conductivity of for pure NiFe_2O_4 nanoparticles. It is observed from the graph that ac conductivity increases with increasing frequency. At low frequency grains boundaries are effective, so electrons can not overcome the barrier, therefore ac conductivity is minimum. While at high frequency area grains become effective,

therefore electrons move easily and ac conductivity show increasing trend. As a result hopping of charge carrier increases with the increase in applied field, therefore the AC conductivity increases[63].

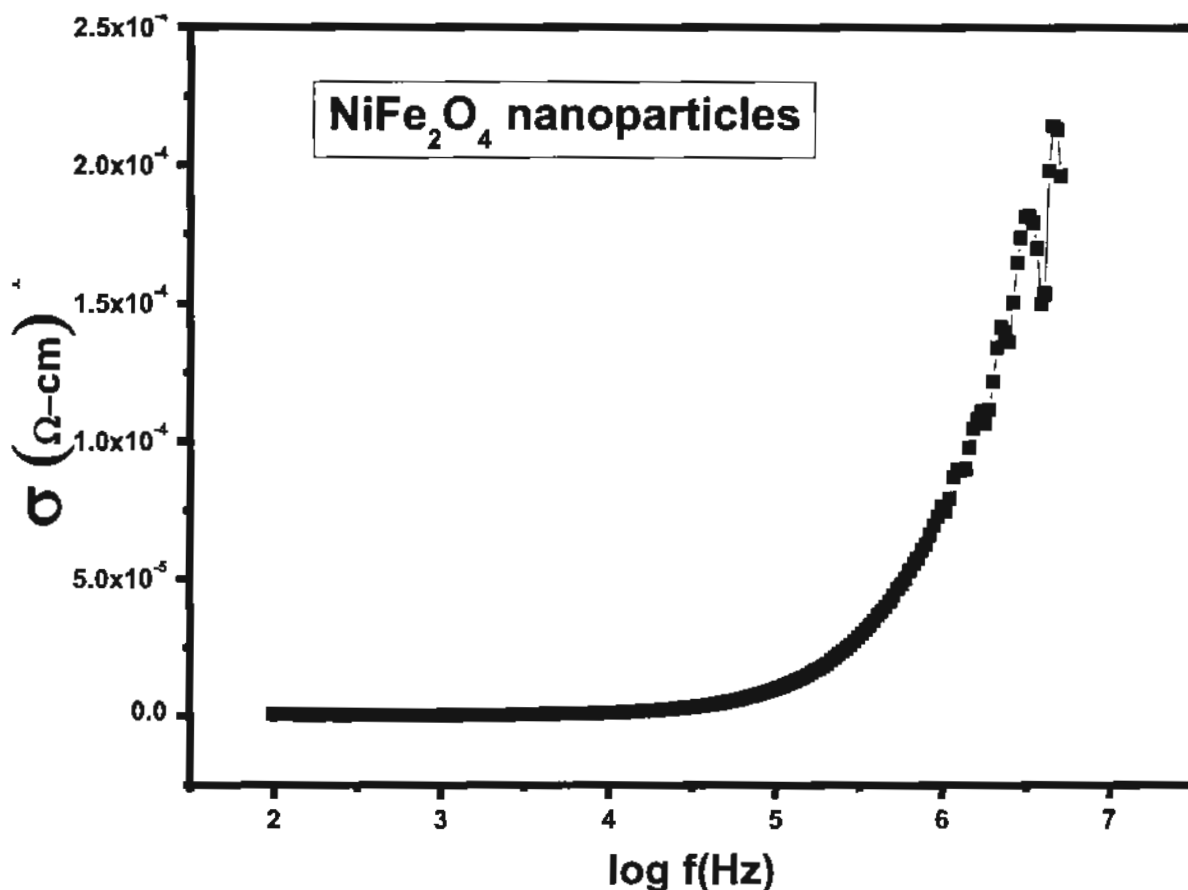
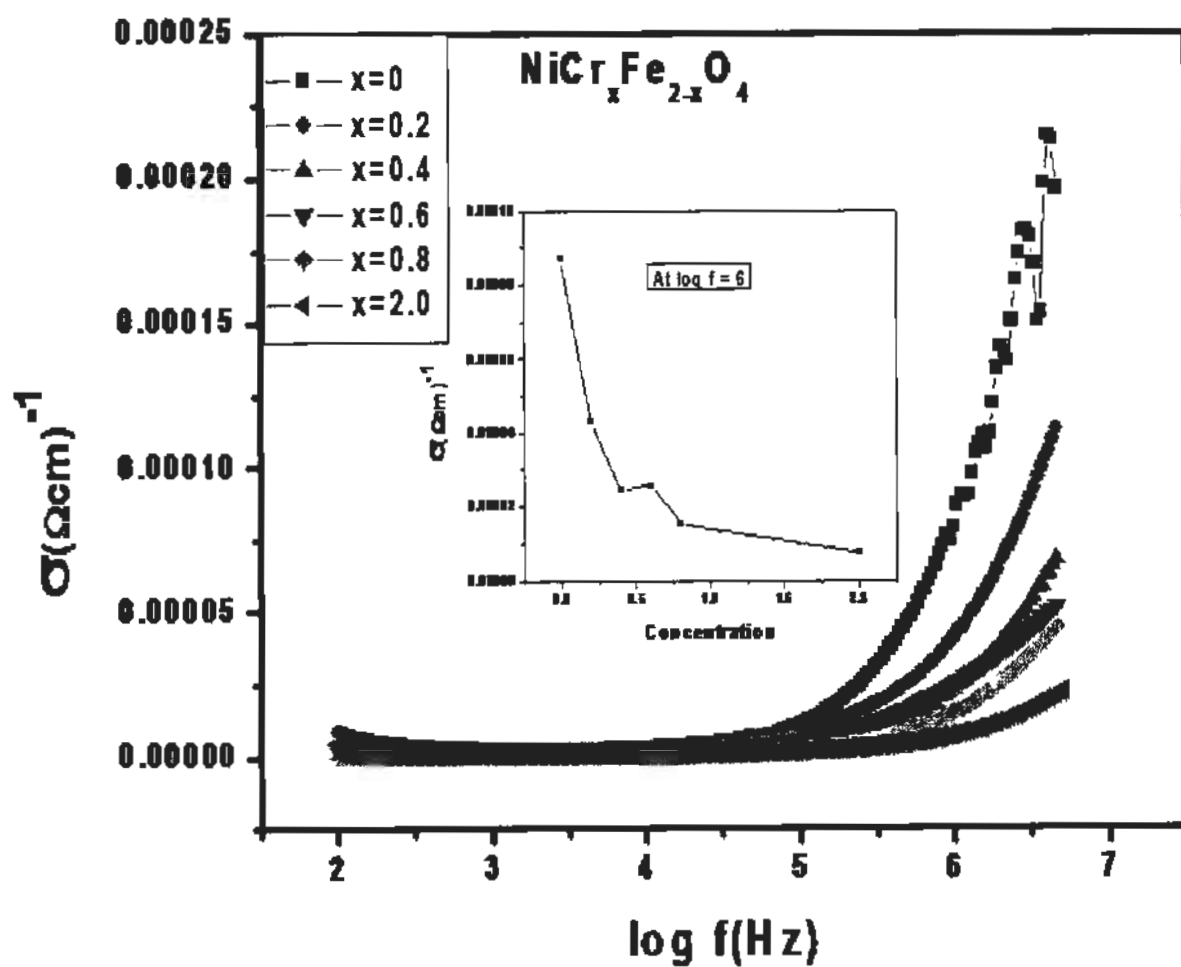


Fig. 4.9(a): AC conductivity of NiFe_2O_4 nanoparticles.

Fig. 4.9(b) shows the ac conductivity of Cr^{3+} doped NiFe_2O_4 nanoparticles. On doping with Cr^{3+} , the ac conductivity has decreased. It is due to the less conductive behavior of chromium as compare to iron. When Cr^{3+} is doped in nickel ferrites at octahedral B-site, then Cr^{3+} ions are taking place of Fe^{3+} , so hopping electrons which take place in conduction are reduced. That's way ac conductivity decreased.

Fig. 4.9(b): AC conductivity of $\text{NiCr}_x\text{Fe}_{2-x}\text{O}_4$.

Conclusions

Cr doped NiFe_2O_4 nanoparticles have been successfully synthesized by sol-gel method. Structural analyses were carried out with the help of XRD, FTIR, EDX and TEM analysis. Dielectric measurements of the investigated samples were studied with the help of LCR meter. XRD patterns revealed that diffraction peaks of all the samples represent the cubic spinel structure. Nanoparticles contained single phase structure with no additional phase. The lattice constant decreases with an increase in Cr contents. The average crystallite size of $\text{NiCr}_x\text{Fe}_{2-x}\text{O}_4$ nanoparticles lies in the 28 nm to 40 nm range. FTIR spectrum revealed that two main absorption bands ν_1 and ν_2 were found in the frequency range $595\text{-}622\text{ cm}^{-1}$ and $400\text{-}500\text{ cm}^{-1}$ respectively. The values of absorption band slightly decreased with increasing Cr content. EDX confirm the formation of NiFe_2O_4 nanoparticles. TEM image was obtained at 100 nm showing hexagonal shaped nanoparticles. Dielectric studies of $\text{NiCr}_x\text{Fe}_{2-x}\text{O}_4$ were carried out in the frequency range of 100 Hz to 5 MHz. The decrease in dielectric constant with frequency is due to decrease in polarization because the dipoles cannot follow up the field variation. It was found that real and imaginary part of dielectric and loss tangent decreased by increasing frequency and become independent at high frequency areas while AC conductivity behavior is inversed. On doping with chromium (Cr^{+3}) on octahedral site the real part, imaginary part and loss tangent increased while AC conductivity decreased with doping.

References

References

- [1] S. Lindsay, Introduction to Nanoscience, Oxford University Press, 2009.
- [2] D.K. Eric, Engines of Creation. The Coming Era of Nanotechnology, Anchor Book, (1986).
- [3] F.H. Khan, Chemical Hazards of Nanoparticles to Human and Environment (a Review), *Orient. J. Chem.*, **29** (2014) 1399-1408.
- [4] H. Birol, C.R. Rambo, M. Guiotoku and D. Hotza, Preparation of Ceramic Nanoparticles Via Cellulose-Assisted Glycine Nitrate Process: A Review, *RSC Adv.*, **3** (2013) 2873-2884.
- [5] A. Gusev, Nanomaterials, Nanostructures, and Nanotechnologies [in Russian], Fizmatlit, Moscow (2005), Google Scholar.
- [6] L. Gu, Functionalized Carbon Nanotubes for Biological Applications, in, Clemson University, 2008.
- [7] T.S. Miller, N. Ebejer, A.G. Güell, J.V. Macpherson and P.R. Unwin, Electrochemistry at Carbon Nanotube Forests: Sidewalls and Closed Ends Allow Fast Electron Transfer, *Chem. Commun.*, **48** (2012) 7435-7437.
- [8] D. Thomas, The Exciton Spectrum of Zinc Oxide, *J. Phys. Chem. Solids*, **15** (1960) 86-96.
- [9] J. Gimzewski and V. Vesna, The Nanoneme Syndrome: Blurring of Fact and Fiction in the Construction of a New Science, *Technoetic arts*, **1** (2003) 7-24.
- [10] K.E. Drexler, Molecular Engineering: An Approach to the Development of General Capabilities for Molecular Manipulation, *Proc. Natl. Acad. Sci.*, **78** (1981) 5275-5278.
- [11] G. Binnig, C.F. Quate and C. Gerber, Atomic Force Microscope, *Phys. Rev. Lett.*, **56** (1986) 930.
- [12] M. Monthieux and V.L. Kuznetsov, Who Should Be Given the Credit for the Discovery of Carbon Nanotubes?, *Carbon*, **44** (2006) 1621-1623.
- [13] P. Malik and A. Sangwan, Nanotechnology: A Tool for Improving Efficiency of Bio-Energy, *J. Eng. Appl. Sci.*, **1** (2012) 37-49.

References

- [14] M. Bruce, Domain Theory, Hitchhiker's Guide to Magnetism for the Environmental Magnetism Workshop, Institute for Rock Magnetism http://www.irm.umn.edu/hg2m/hg2m_d/hg2m_d.html, (1991).
- [15] P. Tsai, Synthesis and Characterization of Ferromagnetic Nanowires, (2011).
- [16] R.C. Smith, Smart Material Systems: Model Development, SIAM, 2005.
- [17] M. Vucinic-Vasic, M. Boskovic, A. Antic, G. Stojanovic, M. Radovanovic, M. Fabian, C. Jovalekic, M.B. Pavlovic and B. Antic, Temperature Induced Evolution of Structure/Microstructure Parameters and Their Correlations with Electric/Magnetic Properties of Nanocrystalline Nickel Ferrite, *Ceram. Int.*, **40** (2014) 4521-4527.
- [18] B. Shirk and W. Buessem, Temperature Dependence of M_s and K_1 of $BaFe_{12}O_{19}$ and $SrFe_{12}O_{19}$ Single Crystals, *J. Appl. Phys.*, **40** (1969) 1294-1296.
- [19] S. Son, M. Taheri, E. Carpenter, V. Harris and M. McHenry, Synthesis of Ferrite and Nickel Ferrite Nanoparticles Using Radio-Frequency Thermal Plasma Torch, *J. Appl. Phys.*, **91** (2002) 7589-7591.
- [20] M.T. Johnson, F.J. Den Broeder and J.W. Smits, Magnetic Device and Method for Locally Controllably Altering Magnetization Direction, in, Google Patents, 1997.
- [21] A.R. Von Hippel, Dielectric Materials and Applications, Artech House on Demand, 1954.
- [22] S. Saafan and S. Assar, Dielectric Behavior of Nano-Structured and Bulk Li Ni Zn Ferrite Samples, *J. Magn. Magn. Mater.*, **324** (2012) 2989-3001.
- [23] M. El Hiti, Dielectric Behaviour in Mg-Zn Ferrites, *J. Magn. Magn. Mater.*, **192** (1999) 305-313.
- [24] R. Usha, A. Sharma and B. Dandapat, Publications and Outreach Activities.
- [25] W.B. Weir, Automatic Measurement of Complex Dielectric Constant and Permeability at Microwave Frequencies, *Proc. of the IEEE.*, **62** (1974) 33-36.
- [26] C. Barathiraja, A. Manikandan, A.U. Mohideen, S. Jayasree and S.A. Antony, Magnetically Recyclable Spinel $Mn_xNi_{1-x}Fe_2O_4$ ($x= 0.0-0.5$) Nano-Photocatalysts: Structural, Morphological and Opto-Magnetic Properties, *J. Supercond. and Nov. Magn.*, **29** (2016) 477-486.

References

- [27] M. Ishaque, M.A. Khan, I. Ali, M. Athair, H.M. Khan, M.A. Iqbal, M. Islam and M.F. Warsi, Synthesis of Nickel–Zinc–Yttrium Ferrites: Structural Elucidation and Dielectric Behavior Evaluation, *Mater. Sci. Semicond. Process.*, **41** (2016) 508-512.
- [28] A.R. Ćosović, T. Žák, S.B. Glisic, M.D. Sokić, S.S. Lazarević, V.R. Ćosović and A.M. Orlović, Synthesis of Nano-Crystalline NiFe₂O₄ Powders in Subcritical and Supercritical Ethanol, *J. Supercrit. Fluids.*, **113** (2016) 96-105.
- [29] R. Choubey, D. Das and S. Mukherjee, Effect of Doping of Manganese Ions on the Structural and Magnetic Properties of Nickel Ferrite, *J. Alloys Compd.*, **668** (2016) 33-39.
- [30] D. Ni, Z. Lin, P. Xiaoling, W. Xinqing and G. Hongliang, Preparation and Characterization of Nickel-Zinc Ferrites by a Solvothermal Method, *Rare. Metal. Mat. Eng.*, **44** (2015) 2126-2131.
- [31] S. Anjum, A. Rashid, F. Bashir, S. Riaz, M. Pervaiz and R. Zia, Effect of Cu-Doped Nickel Ferrites on Structural, Magnetic, and Dielectric Properties, *IEEE Trans. Magn.*, **50** (2014) 1-4.
- [32] I. Polaert, S. Bastien, B. Legras, L. Estel and N. Braidy, Dielectric and Magnetic Properties of NiFe₂O₄ at 2.45 GHz and Heating Capacity for Potential Uses under Microwaves, *J. Magn. Magn. Mater.*, **374** (2015) 731-739.
- [33] H. Moradmard, S.F. Shayesteh, P. Tohidi, Z. Abbas and M. Khaleghi, Structural, Magnetic and Dielectric Properties of Magnesium Doped Nickel Ferrite Nanoparticles, *J. Alloys Compd.*, **650** (2015) 116-122.
- [34] S. Joshi, M. Kumar, S. Chhoker, G. Srivastava, M. Jewariya and V. Singh, Structural, Magnetic, Dielectric and Optical Properties of Nickel Ferrite Nanoparticles Synthesized by Co-Precipitation Method, *J. Mol. Struct.*, **1076** (2014) 55-62.
- [35] H. Arabi and F. Ganjali, Structural and Magnetic Properties of Cobalt and Manganese Doped Ni-Ferrite Nanoparticles, *J. Supercond. and Nov. Magn.*, **26** (2013) 1031-1035.
- [36] G. Dixit, J. Singh, R. Srivastava and H. Agrawal, Structural, Optical and Magnetic Studies of Ce Doped NiFe₂O₄ Nanoparticles, *J. Magn. Magn. Mater.*, **345** (2013) 65-71.

References

- [37] W.-l. JIAO and L. ZHANG, Preparation and Gas Sensing Properties for Acetone of Amorphous Ag Modified NiFe₂O₄ Sensor, *Trans. Nonferrous Met. Soc. China*, **22** (2012) 1127-1132.
- [38] P. Sivakumar, R. Ramesh, A. Ramanand, S. Ponnusamy and C. Muthamizhchelvan, Structural, Thermal, Dielectric and Magnetic Properties of NiFe₂O₄ Nanoleaf, *J. Alloys Compd.*, **537** (2012) 203-207.
- [39] M. Ahmed, S. El-Dek, I. El-Kashef and N. Helmy, Structural and Magnetic Properties of Nano-Crystalline Ag⁺ Doped NiFe₂O₄, *Solid State Sci.*, **13** (2011) 1176-1179.
- [40] M. Airimioaei, C. Ciomaga, N. Apostolescu, L. Leontie, A. Iordan, L. Mitoseriu and M. Palamaru, Synthesis and Functional Properties of the Ni_{1-x}Mn_xFe₂O₄ Ferrites, *J. Alloys Compd.*, **509** (2011) 8065-8072.
- [41] C. Giacovazzo, *Fundamentals of Crystallography*, Oxford university press, USA, 2002.
- [42] B. Cullity, *Elements of X-Ray Diffraction 2nd Edition*. Addison-Wesley Pub. Co, Inc, CA, USA, **197** (1978) 356.
- [43] B. Warren and X.-r. Diffraction, Courier Dover Publications, New York, (1969).
- [44] V.K. Pecharsky and P.Y. Zavalij, *Fundamentals of Powder Diffraction and Structural Characterization of Materials*, Springer, 2009.
- [45] C. Ammer, D.S. Ammer, C. Anderegg and J.G. Barlow, *Books, Journals, and Newspapers*, DREW, **11** (1982) 139.
- [46] P.R. Griffiths and J.A. De Haseth, *Fourier Transform Infrared Spectrometry*, John Wiley & Sons, 2007.
- [47] M. De Graef, *Introduction to Conventional Transmission Electron Microscopy*, Cambridge University Press, 2003.
- [48] D.B. Williams, C.B. Carter and P. Veysiere, *Transmission Electron Microscopy: A Textbook for Materials Science*, Springer, 1998.
- [49] P.H. Holloway, *Characterization of Metals and Alloys*, Momentum Press, 2009.
- [50] M. Atmanand, V.J. Kumar and V.G. Murti, A Microcontroller-Based Quasi-Balanced Bridge for the Measurement of L, C and R, *IEEE Trans. Instru. and Measur.*, **45** (1996) 757-761.

References

- [51] M. Kamran, A. Ullah, S. Rahman, A. Tahir, K. Nadeem, M.A. ur Rehman and S. Hussain, Structural, Magnetic, and Dielectric Properties of Multiferroic $\text{Co}_{1-x}\text{Mg}_x\text{Cr}_2\text{O}_4$ Nanoparticles, *J. Magn. Magn. Mater.*, **433** (2017) 178-186.
- [52] T. Shinde, A. Gadkari and P. Vasambekar, Dc Resistivity of Ni-Zn Ferrites Prepared by Oxalate Precipitation Method, *Mater. Chem. Phys.*, **111** (2008) 87-91.
- [53] P. Luo and T. Nieh, Preparing Hydroxyapatite Powders with Controlled Morphology, *Biomaterials*, **17** (1996) 1959-1964.
- [54] E. El-Ghazzawy and S. Alamri, Ni_xFe_{2-x}O₄ Ferrite Nanoparticles and Their Composites with Polypyrrole: Synthesis, Characterization and Magnetic Properties, *Bull. Mater. Sci.*, **38** (2015) 915-924.
- [55] M. Sertkol, Y. Köseoğlu, A. Baykal, H. Kavas, A. Bozkurt and M.S. Toprak, Microwave Synthesis and Characterization of Zn-Doped Nickel Ferrite Nanoparticles, *J. Alloys Compd.*, **486** (2009) 325-329.
- [56] J. Lu, X. Jiao, D. Chen and W. Li, Solvothermal Synthesis and Characterization of Fe₃O₄ and Γ -Fe₂O₃ Nanoplates, *J. Phys. Chem. C*, **113** (2009) 4012-4017.
- [57] D. Han, J. Wang and H. Luo, Crystallite Size Effect on Saturation Magnetization of Fine Ferrimagnetic Particles, *J. Magn. Magn. Mater.*, **136** (1994) 176-182.
- [58] C. Koops, On the Dispersion of Resistivity and Dielectric Constant of Some Semiconductors at Audiofrequencies, *Phys. Rev.*, **83** (1951) 121.
- [59] T. Krieg and D.J. Mogul, Transcranial Magnetic Stimulation, in: *Neural Engineering*, Springer, (2013) pp. 405-453.
- [60] K. Wagner, *Etz* 32. Iooi—02. 1911; 33. 6, 55—37.> 912; 86. 606—609, 601—24.'95-Ann. D. Phys.,**40** (1913) 817-855.
- [61] J. Malmivuo and R. Plonsey, *Bioelectromagnetism: Principles and Applications of Bioelectric and Biomagnetic Fields*, Oxford University Press, USA, 1995.
- [62] K. Nadeem, L. Ali, I. Gul, S. Rizwan and M. Mumtaz, Effect of Silica Coating on the Structural, Dielectric, and Magnetic Properties of Maghemite Nanoparticles, *J. Non-Cryst. Solids*, **404** (2014) 72-77.
- [63] E. Verwey, P. Haayman and F. Romeijn, Physical Properties and Cation Arrangement of Oxides with Spinel Structures II. Electronic Conductivity, *J. Chem. Phys.*, **15** (1947) 181-187.